University of Groningen

Algorithms for computing normally hyperbolic invariant manifolds

Broer, H.W.; Osinga, H.M.; Vegter, G.

IMPORTANT NOTE: You are advised to consult the publisher's version (publisher's PDF) if you wish to cite from it. Please check the document version below.

Document Version
Publisher's PDF, also known as Version of record

[Link to publication in University of Groningen/UMCG research database](#)

Citation for published version (APA):
Broer, H. W., Osinga, H. M., & Vegter, G. (1997). Algorithms for computing normally hyperbolic invariant manifolds. *Zeitschrift für Angewandte Mathematik und Mechanik*, *48*(3), 480-524.

Algorithms for computing normally hyperbolic invariant manifolds

H. W. Broer, H. M. Osinga[1] and G. Vegter

Abstract. An efficient algorithm is developed for the numerical computation of normally hyperbolic invariant manifolds, based on the graph transform and Newton's method. It fits in the perturbation theory of discrete dynamical systems and therefore allows application to the setting of continuation. A convergence proof is included. The scope of application is not restricted to hyperbolic attractors, but extends to normally hyperbolic manifolds of saddle type. It also computes stable and unstable manifolds. The method is robust and needs only little specification of the dynamics, which makes it applicable to e.g. Poincaré maps. Its performance is illustrated on examples in 2D and 3D, where a numerical discussion is included.

Mathematics Subject Classification (1991). 34C30, 58F35, 58F15.

Keywords. Dynamical systems, invariant manifolds, normal hyperbolicity, stable and unstable manifolds, graph transform, constructive proofs, algorithms, Newton's method, numerical experiments.

1. Introduction

Invariant manifolds play an important role in the qualitative analysis of dynamical systems. This paper focuses on normally hyperbolic manifolds, like closed orbits, invariant tori and their stable and unstable manifolds.

Methods dealing with special cases have been around for some time. The first general method, based on the *graph transform*, was developed by Hirsch, Pugh and Shub in [10]. Normal hyperbolicity guarantees that the graph transform is a contraction on a space of embeddings, its fixed point corresponding to the desired invariant manifold. For related work on invariant manifolds and hyperbolic dynamical systems we refer to Palis and Takens [15], Ruelle [16], and Shub [17].

The graph transform method is *constructive*, and therefore provides a basis for the development of an algorithm, executable on a computer. However, the context of the graph transform involves geometric objects like manifolds, maps and

---

bundles. The main problem is to provide finite representations for these objects. Such representations, necessary for manipulation by a computer, are introduced in this paper, and the graph transform method is adapted accordingly. A similar program, for the computation of stable and unstable manifolds of hyperbolic fixed points, is developed in Homburg, Osinga and Vegter [12].

Section 2.1 contains a brief review of the Invariant Manifold Theorem [10]. We restrict ourselves to diffeomeorphisms whose domain is an open subset of $\mathbb{R}^d$, see section 2.2. In this context we design an algorithm that has a straightforward implementation, and yet covers many interesting applications.

Section 3 describes a special version of the algorithm in the simple case of absence of normal expansion. It presents the *graph transform* as a key ingredient of the algorithm, see section 3.1. The graph transform, associated with the diffeomorphism f_ε, may be considered as a contraction, defined on the space of embeddings of H_0 in $\mathbb{R}^d$. (For brevity's sake we are cheating a little here, since the graph transform is actually defined on the space of sections of a certain normal bundle.) Its fixed point is an embedding, whose image $\mathbb{H}_\varepsilon$ is the invariant manifold of f_ε. The image of an embedding under the graph transform is defined, however, in terms of an implicit equation. To solve this equation efficiently we first derive a global version of Newton's method in section 3.2, that may be of some independent significance. This rather general method is applied to the computation of the normally hyperbolic invariant manifold $\mathbb{H}_\varepsilon$ of f_ε in section 3.3, that also contains rather precise estimates concerning the speed of convergence of the algorithm. The computation of the Df_ε–invariant splitting of the tangent bundle (see section 2.2 for a definition) along $\mathbb{H}_\varepsilon$ is described in section 3.4. We also indicate how our algorithm can be used to compute invariant manifolds in a continuation context, where the parameter ε ranges over an interval that is not necessarily small, see section 3.5. This setting arises frequently in applications.

After a brief description of some special features of the algorithm in the absence of normal contraction, see section 4, we sketch the general case in section 5. Here we describe the computation of the normally hyperbolic invariant manifold, and its stable and unstable manifolds, when both normal expansion and normal contraction are present. Section 7 contains some numerical examples, illustrating the method first in the simple case of absence of normal expansion, see section 7.1, and subsequently in the general case, see section 7.2. Finally, we show, in section 7.3, how to apply the method to compute the invariant manifold of the Poincaré first–return map of a continuous system. More examples can be found in Osinga [14], which also contains an extensive survey of related literature.

2. Normally hyperbolic submanifolds

2.1. The Invariant Manifold Theorem

First we present an overview of some basic definitions and results from [10]. Consider a C^K diffeomorphism f_0 on a C^K manifold M, having a K–normally hyperbolic invariant manifold $H_0 \subset M$. Recall that H_0 is K–normally hyperbolic for f_0, $K \geq 1$, if there is a continuous Df_0–invariant splitting

$$T_{H_0}(M) = N^u(H_0) \oplus T_{H_0} \oplus N^s(H_0),$$

and a Riemannian structure on the tangent bundle $T_{H_0}(M)$, such that, for $r \in H_0$ and $0 \leq k \leq K$:

$$\begin{aligned}
\|Df_0 \mid N^s_r(H_0)\| \cdot \|(Df_0 \mid T_r(H_0))^{-1}\|^k &< 1, \\
\|(Df_0 \mid N^u_r(H_0))^{-1}\| \cdot \|Df_0 \mid T_r(H_0)\|^k &< 1.
\end{aligned} \tag{1}$$

Here the norms are associated with the Riemann structure on $T_{H_0}(M)$.

According to the *Invariant Manifold Theorem* a C^K diffeomorphism f, that is C^K–near f_0, has a K–normally hyperbolic invariant manifold H, that is C^K and C^K–near H_0. In particular, there is a continuous Df–invariant splitting $T_H(M) = N^u(H) \oplus T(H) \oplus N^s(H)$, of the tangent bundle $T_H(M)$. Our primary goal is the computation of both H and the invariant splitting of $T_H(M)$. Furthermore the Invariant Manifold Theorem states that, for some neighborhood U of H, the sets

$$W^s(H) = \bigcap_{n \geq 0} f^{-n}(U) \ \text{ and } \ W^u(H) = \bigcap_{n \geq 0} f^n(U)$$

are C^K submanifolds of M, tangent to $T_r(H) \oplus N^s_r(H)$ and $N^u_r(H) \oplus T_r(H)$, at $r \in H$. These manifolds, called the *stable* and *unstable* manifolds of H, can also be computed using the method developed in this paper, as we describe briefly in section 5.2. In this paper we assume, for technical reasons, that $K \geq 3$.

2.2. Normally hyperbolic submanifolds of $\mathbb{R}^d$

Let $f_0 : U \subset \mathbb{R}^d \to \mathbb{R}^d$ be a diffeomorphism, defined on an open subset U of $\mathbb{R}^d$, having a 1–normally hyperbolic invariant manifold $H_0 \subset U$. (We usually write $f_0 : \mathbb{R}^d \to \mathbb{R}^d$, even though in general U is a proper subset of $\mathbb{R}^d$.) We assume throughout this paper that H_0 is compact. In this section we describe how to represent the geometric objects that show up in the computation of invariant manifolds, taking advantage of the fact that the ambient manifold is a euclidean space.
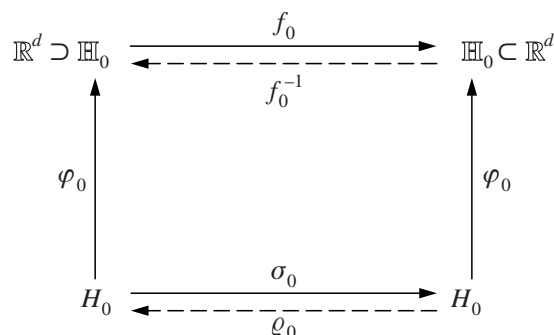
$$\mathbb{R}^d \supset \mathbb{H}_0 \quad \underset{f_0^{-1}}{\overset{f_0}{\longleftarrow}} \quad \mathbb{H}_0 \subset \mathbb{R}^d$$

$$\varphi_0 \uparrow \qquad\qquad\qquad \uparrow \varphi_0$$

$$H_0 \quad \underset{\varrho_0}{\overset{\sigma_0}{\longleftarrow}} \quad H_0$$

Figure 1.
The abstract manifold H_0 and its embedding in $\mathbb{R}^d$.

Representation of the invariant manifold

Let $\varphi_0 : H_0 \to \mathbb{R}^d$ be the canonical embedding of H_0. We distinguish between the *abstract manifold* H_0, and its *image* $\varphi_0(H_0)$, which is a submanifold of $\mathbb{R}^d$. To stress this distinction, we denote $\varphi_0(H_0)$ by $\mathbb{H}_0$. The tangent space $T_{\varphi_0(r)}(\varphi_0(H_0))$ can be identified with an *affine* subspace of $\mathbb{R}^d$ of the form $\varphi_0(r) + \mathbb{T}_r(\mathbb{H}_0)$, where $\mathbb{T}_r(\mathbb{H}_0)$ is a *linear* subspace of $\mathbb{R}^d$. Since f_0 leaves $\mathbb{H}_0$ invariant, there is a diffeomorphism $\sigma_0 : H_0 \to H_0$ such that $f_0(\varphi_0(r)) = \varphi_0(\sigma_0(r))$, for $r \in H_0$. Its inverse is denoted by ϱ_0. Note that σ_0 and ϱ_0 may be regarded as the restriction of f_0 and f_0^{-1} to $\mathbb{H}_0$, respectively. See also figure 1. Although the distinction between the abstract manifold H_0 and its φ_0–image $\mathbb{H}_0$ in $\mathbb{R}^d$ involves rather extensive notation, our intention to develop algorithms that manipulate geometric objects like manifolds, maps, and bundles, requires that we are quite specific about the representation of these objects. If e.g. $\mathbb{H}_0 \subset \mathbb{R}^d$ the 'user' of the algorithm may choose to represent points on H_0 by their coordinates in $\mathbb{R}^d$, in which case φ_0 is the inclusion map of H_0 in $\mathbb{R}^d$. However, in some applications it may be more natural to represent the manifold H_0 by coordinates that are adapted to the dynamics of f_0 on H_0, like the case in which H_0 is a (higher–dimensional) torus, represented by angular coordinates.

Representation of normal bundles

The restricted context, in which the ambient manifold is $\mathbb{R}^d$, enables us to identify neighborhoods of the 0-sections the stable and unstable normal bundles of H_0 with certain subsets of $\mathbb{R}^d$. To see this, let the dimension of H_0 be denoted by c, and the dimension of the fibers of the bundles $N^s(H_0)$ and $N^u(H_0)$ by s and u, respectively. In particular, $c + s + u = d$. As observed above, for $r \in H_0$, the space $T_r(H_0)$ corresponds to the affine subspace $\varphi_0(r) + \mathbb{T}_r(\mathbb{H}_0)$ of $\mathbb{R}^d$. Similarly $N_r^s(H_0)$ and $N_r^u(H_0)$ correspond to affine subspaces of $\mathbb{R}^d$, going through the point $\varphi_0(r) \in \mathbb{H}_0$.

They are, therefore, of the form $\varphi_0(r) + \mathbb{N}_r^s(\mathbb{H}_0)$ and $\varphi_0(r) + \mathbb{N}_r^u(\mathbb{H}_0)$, respectively, where $\mathbb{N}_r^s(\mathbb{H}_0)$ and $\mathbb{N}_r^u(\mathbb{H}_0)$ are s–dimensional and u–dimensional linear subspaces of $\mathbb{R}^d$. We identify $T_{\varphi_0(r)}(\mathbb{R}^d)$ with $\mathbb{T}_r(\mathbb{H}_0) \oplus \mathbb{N}_r^s(\mathbb{H}_0) \oplus \mathbb{N}_r^u(\mathbb{H}_0)$. Finally

$$\Pi_r^c : \mathbb{R}^d \to \mathbb{T}_r(\mathbb{H}_0), \ \ \Pi_r^s : \mathbb{R}^d \to \mathbb{N}_r^s(\mathbb{H}_0) \ \ \text{and} \ \ \Pi_r^u : \mathbb{R}^d \to \mathbb{N}_r^u(\mathbb{H}_0) \tag{2}$$

are the canonical projections.

The Riemannian metric on $\mathbb{R}^d$ (in terms of which normal hyperbolicity is defined — see (1)) induces an inner product on the spaces $\mathbb{T}_r(\mathbb{H}_0)$, $\mathbb{N}_r^s(\mathbb{H}_0)$ and $\mathbb{N}_r^u(\mathbb{H}_0)$. We represent this pointwise inner product by bases, consisting of vectors in $\mathbb{R}^d$, that are by definition orthonormal with respect to the Riemannian structure. More specifically, consider an orthonormal basis $v_1^s(r), \cdots, v_s^s(r)$ of $\mathbb{N}_r^s(\mathbb{H}_0)$, for $r \in H_0$. Note that in general the vector valued functions $v_i^s : H_0 \to \mathbb{R}^d$ are not globally continuous, since this amounts to triviality of the normal bundle $N^s(H_0)$. However, in this paper we make the following assumption:

Assumption 1 (Triviality of normal bundles). *There are C^0 functions $v_1^s, \cdots, v_s^s : H_0 \to \mathbb{R}^d$ such that $v_1^s(r), \cdots, v_s^s(r)$ form a basis of $\mathbb{N}_r^s(\mathbb{H}_0)$, for $r \in H_0$. Similarly, there are C^0 functions $v_1^u, \cdots, v_u^u : H_0 \to \mathbb{R}^d$ such that $v_1^u(r), \cdots, v_u^u(r)$ form a basis of $\mathbb{N}_r^u(\mathbb{H}_0)$, for $r \in H_0$. Moreover, we may even assume that these bases are orthonormal with respect to the Riemannian metric.*

The identification map $\iota_r^s : \mathbb{N}_r^s(\mathbb{H}_0) \to \mathbb{R}^s$ is defined by

$$\iota_r^s \Big(\sum_{i=1}^{s} \eta_i^s v_i^s(r) \Big) = (\eta_1^s, \cdots, \eta_s^s). \tag{3}$$

The identification map $\iota_r^u : \mathbb{N}_r^u(\mathbb{H}_0) \to \mathbb{R}^u$ is defined similarly.

Due to the triviality of the normal bundle the manifold H_0 has a neighborhood in $\mathbb{R}^d$ that is diffeomorphic to $H_0 \times \mathbb{R}^s \times \mathbb{R}^u$. More precisely, the map $\Phi : H_0 \times \mathbb{R}^s \times \mathbb{R}^u \to \mathbb{R}^d$, defined by

$$\Phi(r, \eta^s, \eta^u) = \varphi_0(r) + \sum_{i=1}^{s} \eta_i^s v_i^s(r) + \sum_{i=1}^{u} \eta_i^u v_i^u(r),$$

is a diffeomorphism from a neighborhood of $H_0 \times \{0\} \times \{0\}$ to a neighborhood of $\mathbb{H}_0$ in $\mathbb{R}^d$. Note that $\Phi(\{r\} \times \mathbb{R}^s \times \{0\}) = \varphi_0(r) + \mathbb{N}_r^s(\mathbb{H}_0)$, and $\Phi(\{r\} \times \{0\} \times \mathbb{R}^u) = \varphi_0(r) + \mathbb{N}_r^u(\mathbb{H}_0)$. The maps $\pi_c : \mathbb{R}^d \to H_0$, $\pi_s : \mathbb{R}^d \to \mathbb{R}^s$ and $\pi_u : \mathbb{R}^d \to \mathbb{R}^u$ are defined on a neighborhood of $\mathbb{H}_0$ by mapping inverse images under Φ onto H_0, $\mathbb{R}^s$ and $\mathbb{R}^u$, respectively, under the canonical projections. In this way we identify the stable normal bundle $N^s(H_0)$ with the space $H_0 \times \mathbb{R}^s$, and the unstable normal bundle $N^u(H_0)$ with $H_0 \times \mathbb{R}^u$. Therefore it is justifiable to refer to maps $\eta^s : H_0 \to \mathbb{R}^s$ and $\eta^u : H_0 \to \mathbb{R}^u$ as *sections*. With a pair of sections (η^s, η^u) we associate

the *embedding* $\varphi : H_0 \to \mathbb{R}^d$, defined by $\varphi(r) = \Phi(r, \eta^s(r), \eta^u(r))$. In particular, the embedding φ_0 is associated with the 0–sections of the normal bundles. If f_0 is defined on a manifold other than $\mathbb{R}^d$, or if the normal bundles are not trivial, the methods of this paper still apply. However, the need for local coordinates introduces more complicated (multiple) representations of the geometric objects the algorithm manipulates; cf [16] for a proof of the Invariant Manifold Theorem along these lines. A different approach can be found in [10], where the exponential map, associated with the Riemannian metric, is used to identify a neighborhood of the 0–section in the normal bundle with a neighborhood of $\mathbb{H}_0$ in the ambient manifold. It seems hard to turn the latter method into an efficient algorithm.

Representation of derivatives

In computations it is important to have explicit representations for the *derivative* of e.g. f_0 in points of $\mathbb{H}_0$, cf (1). Since the linear spaces $\mathbb{N}_r^s(\mathbb{H}_0)$, $r \in H_0$, form a Df_0–invariant family, there are *globally defined* C^{K-1} functions $\kappa_{ij}^s : H_0 \to \mathbb{R}$, $1 \le i, j \le s$, such that

$$Df_0(\varphi_0(r))(v_i^s(r)) = \sum_{j=1}^{s} \kappa_{ij}^s(r) v_j^s(\sigma_0(r)),$$

for $i = 1, \cdots, s$. Let $K_0^s(r)$ be the $s \times s$ matrix with entries $\kappa_{ij}^s(r)$. Similarly there are C^{K-1} functions $\kappa_{ij}^u : H_0 \to \mathbb{R}$, $1 \le i, j \le u$, such that

$$Df_0(\varphi_0(r))(v_i^u(r)) = \sum_{j=1}^{s} \kappa_{ij}^u(r) v_j^u(\sigma_0(r)),$$

for $i = 1, \cdots, u$. Let $K_0^u(r)$ be the $u \times u$ matrix with entries $\kappa_{ij}^u(r)$. Then *0–normal hyperbolicity* of $\mathbb{H}_0$ boils down to $\lambda^s := \sup_{r \in H_0} \|K_0^s(r)\| < 1$, and $\lambda^u := \sup_{r \in H_0} \|K_0^u(r)^{-1}\| < 1$. Here we take the matrix norm with respect to the standard inner product on $\mathbb{R}^s$ and $\mathbb{R}^u$, respectively. Although the matrices $K_0^s(r)$ and $K_0^u(r)$ do depend on the particular choice of the functions v_i^s, $1 \le i \le s$, and v_i^u, $1 \le i \le u$, their norms are independent of this choice.

To express *1–normal hyperbolicity*, let $v_1^c(r), \cdots, v_c^c(r)$ span the tangent space $\mathbb{T}_r(\mathbb{H}_0)$. (Note that in general v_i^c is not globally continuous, since this would amount to parallellizability of $\mathbb{H}_0$.) Since $\mathbb{H}_0$ is f_0–invariant, there are locally defined $\alpha_{ij}(r) \in \mathbb{R}$, $1 \le i, j \le c$, such that

$$Df_0(\varphi_0(r))(v_i^c(r)) = \sum_{j=1}^{c} \alpha_{ij}(r) v_j^c(\sigma_0(r)),$$

for $i = 1, \cdots, c$. Let $A_0(r)$ be the $c \times c$–matrix with entries $\alpha_{ij}(r)$. Then $\mu^s := \sup_{r \in H_0} \|K_0^s(r)\| \|A_0(r)^{-1}\| < 1$, and $\mu^u := \sup_{r \in H_0} \|K_0^u(r)^{-1}\| \|A_0(r)\| < 1$, since $\mathbb{H}_0$ is a 1–normally hyperbolic invariant manifold for f_0.

Perturbation context

We study diffeomorphisms on $\mathbb{R}^d$ that are C^K–near f_0 ($K \geq 3$). More specifically, we restrict to a *perturbation context* in which these diffeomorphisms occur in a C^K family $f : \mathbb{R}^d \times \mathbb{R} \to \mathbb{R}^d$, such that $f_0(p) = f(p, 0)$, for $p \in \mathbb{R}^d$.

In this setting families of embeddings, sections of bundles, etc., are maps $g : X \times \mathbb{R} \to Y$, depending on $(x, \varepsilon) \in X$. Here $\varepsilon \in \mathbb{R}$ is considered as a parameter, ranging over some neighborhood of $0 \in \mathbb{R}$. Individual members of a family like g are denoted by subscripting the family name with the parameter name, e.g. $g_\varepsilon(x) = g(x, \varepsilon)$. This convention applies throughout the paper.

3. Special case I: absence of normal expansion

In this section we develop an algorithm for the computation of the invariant manifold in the special case of absence of normal expansion, viz $N^u(H_0) = 0$. If no confusion is possible we drop the superscript s from our notation, by writing e.g. $K_0(r)$, $\kappa_{ij}(r)$, λ, ι_r instead of $K_0^s(r)$, $\kappa_{ij}^s(r)$, λ^s, ι_r^s, etc.

3.1. The graph transform

Our goal is to obtain the normally hyperbolic invariant manifold $\mathbb{H}_\varepsilon$ for f_ε by constructing an embedding $\varphi_\varepsilon : H_0 \to \mathbb{R}^d$ with $\mathbb{H}_\varepsilon = \varphi_\varepsilon(H_0)$. We follow [10], by considering special embeddings associated with sections $\eta_\varepsilon : H_0 \to \mathbb{R}^s$ according to $\varphi_\varepsilon(r) = \Phi(r, \eta_\varepsilon(r))$.

The graph of a section $\eta : H_0 \to \mathbb{R}^s$ is the subset $\text{graph}(\eta)$ of $\mathbb{R}^d$, defined by $\text{graph}(\eta) = \{\Phi(r, \eta(r)) \mid r \in H_0\}$. The *graph transform* Γ_{f_ε} is uniquely determined by the condition that it maps a section $h_\varepsilon : H_0 \to \mathbb{R}^s$ onto a section $\eta_\varepsilon : H_0 \to \mathbb{R}^s$, such that $f_\varepsilon(\text{graph}(h_\varepsilon)) = \text{graph}(\eta_\varepsilon)$. In other words, there is a unique point $\varrho \in H_0$ such that the point $\Phi(r, \eta(r, \varepsilon))$ is of the form $f(\Phi(\varrho, h(\varrho, \varepsilon)), \varepsilon)$. It is convenient to express the dependence of ϱ on r and ε by writing $\varrho = \varrho(r, \varepsilon)$. Note that we suppress the dependence of ϱ on h in our notation. We define the graph transform Γ_f on families of sections, i.e. we take $\Gamma_f(h)(r, \varepsilon) = \Gamma_{f_\varepsilon}(\eta_\varepsilon)(r)$. Let $\Sigma(\varepsilon_0)$ be the space of continuous families of sections $h : H_0 \times [-\varepsilon_0, \varepsilon_0] \to \mathbb{R}^s$, with $h(r, 0) = 0$ for $r \in H_0$. Since $\mathbb{H}_0$ is f_0–invariant, the 0–section is a fixed point of Γ_{f_0}, and hence $\Sigma(\varepsilon_0)$ is invariant under Γ_f, provided ε_0 is sufficiently small.

For $h \in \Sigma(\varepsilon_0)$ the family $\eta = \Gamma_f(h)$ is the second component of the solution $(\varrho(r, \varepsilon), \eta(r, \varepsilon))$ of the equation

$$F(\varrho, \eta, r, \varepsilon) = 0, \tag{4}$$

where $F : H_0 \times \mathbb{R}^s \times H_0 \times \mathbb{R} \to \mathbb{R}^d$ is defined by

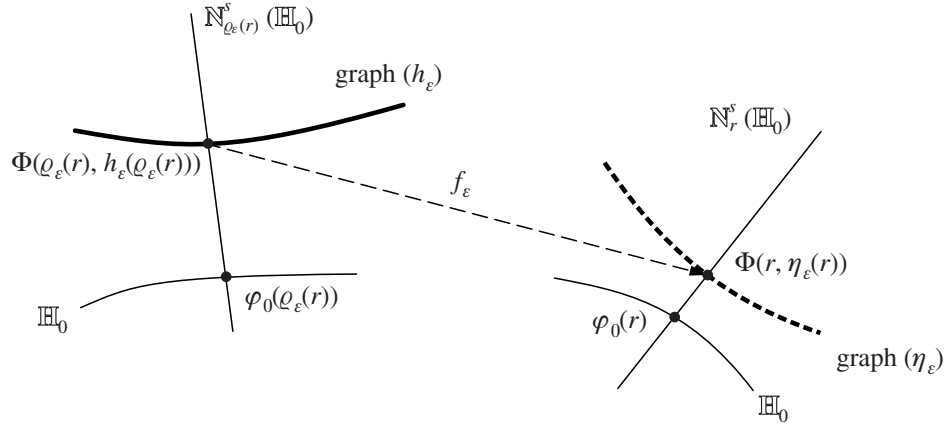$$F(\varrho, \eta, r, \varepsilon) = f(\Phi(\varrho, h(\varrho, \varepsilon)), \varepsilon) - \Phi(r, \eta). \tag{5}$$

Figure 2.
The graph transform Γ_{f_ε} maps h_ε onto η_ε. Its fixed point $\overline{h}_\varepsilon$ defines an embedding $\varphi_\varepsilon : H_0 \to \mathbb{R}^d$ by $\varphi_\varepsilon(r) = \Phi(r, \overline{h}_\varepsilon(r))$, whose image $\mathbb{H}_\varepsilon$ is the normally hyperbolic invariant manifold of f_ε.

See also figure 2.

Note that F is defined on a neighborhood of the subset

$$\{(\varrho_0(r), 0, r, 0) \mid r \in H_0\}.$$

Since $\pi_c \Phi(r, \eta) = r$, the solution of equation (4) can be obtained by first solving $\varrho = \varrho(r, \varepsilon)$ from the equation

$$\sigma(\varrho, \varepsilon) = r, \tag{6}$$

where $\sigma : H_0 \times \mathbb{R} \to H_0$ is defined by

$$\sigma(\varrho, \varepsilon) = \pi_c f(\Phi(\varrho, h(\varrho, \varepsilon)), \varepsilon). \tag{7}$$

In other words: $\varrho_\varepsilon : H_0 \to H_0$ is the inverse of $\sigma_\varepsilon : H_0 \to H_0$. Then η is defined by

$$\eta(r, \varepsilon) = \pi_s f(\Phi(\varrho(r, \varepsilon), h(\varrho(r, \varepsilon), \varepsilon)), \varepsilon).$$

Using the fact that $h(\varrho, 0) = 0$ for $h \in \Sigma(\varepsilon_0)$, we see that

$$\sigma(\varrho, 0) = \pi_c f(\Phi(\varrho, 0), 0) = \pi_c f_0(\varphi_0(\varrho)) = \sigma_0(\varrho).$$

Consequently $\varrho(r, 0) = \varrho_0(r)$.

Equation (6) can be solved by introducing local coordinates on H_0 near $\varrho_0(r)$ and r, and by numerically constructing a solution, viz a local inverse to σ_ε, in terms of these local coordinates. However, we prefer to obtain η *globally*, exploiting the fact that we have identified the bundle $N^s(H_0)$ with a neighborhood of $\mathbb{H}_0$ in $\mathbb{R}^d$

under the mapping Φ. To this end we transform equation (4) into an equation of the form

$$G(y, r, \varepsilon) = 0, \tag{8}$$

where $G : \mathbb{R}^d \times H_0 \times \mathbb{R} \to \mathbb{R}^d$ is a C^K function, $K \geq 3$, defined on a neighborhood of $\varphi_0 H_0 \times H_0 \times \{0\}$, that satisfies, for $r \in H_0$:

$$G(\varphi_0(r), r, 0) = 0.$$

We construct G in section 3.3, but first we develop a global version of Newton's method for solving equations of the form (8).

3.2. A global version of Newton's method

In this section we develop a rather general method for solving equations of the form (8). This method, which may be considered as a global version of Newton's method for determining implicitly defined functions, may be of some independent significance. In this paper it provides a key subroutine for the algorithms that compute the normally hyperbolic submanifold and its stable and unstable manifolds.

First we consider in more detail the spaces of functions we are working with. In this general setting we consider a C^K function, $K \geq 3$, $G : \mathbb{R}^d \times H_0 \times \mathbb{R} \to \mathbb{R}^d$, and a C^K function $\overline{y}_0 : H_0 \to \mathbb{R}^d$ satisfying, for $r \in H_0$,

$$G(\overline{y}_0(r), r, 0) = 0, \quad D_y G(\overline{y}_0(r), r, 0) \text{ is invertible.} \tag{9}$$

(In our case $\overline{y}_0 = \varphi_0$.) Here $D_y G(\overline{y}_0(r), r, 0)$ is the restriction of the derivative $DG(\overline{y}_0(r), r, 0)$ to the space $T_{\overline{y}_0(r)}(\mathbb{R}^d) \times \{0\} \times \{0\}$; We denote this map by $L(r)$.

Note that the solution of equation (8) is a function $H_0 \times \mathbb{R} \to \mathbb{R}^d$, defined on a neighborhood of $H_0 \times \{0\}$, and near $\overline{y}_0$. The Newton operator $\mathcal{N}$ starts with such a function, and computes a better approximation to the solution of (8). More specifically, consider the Banach space $\mathcal{B}(\varepsilon_0)$ of continuous functions $y : H_0 \times [-\varepsilon_0, \varepsilon_0] \to \mathbb{R}^d$, endowed with the sup–norm, viz

$$\|y\| = \sup_{r \in H_0, |\varepsilon| \leq \varepsilon_0} |y(r, \varepsilon)|.$$

Here $|y(r, \varepsilon)|$ is the length of $y(r, \varepsilon) \in \mathbb{R}^d$ with respect to the standard inner product on $\mathbb{R}^d$. We consider $\overline{y}_0$ as an element of this space by identifying it with the map $(r, \varepsilon) \mapsto \overline{y}_0(r)$. The Newton operator $\mathcal{N}$ is defined on $\mathcal{B}(\varepsilon_0)$ by

$$\mathcal{N}y(r, \varepsilon) = y(r, \varepsilon) - L(r)^{-1} \cdot G(y(r, \varepsilon), r, \varepsilon).$$

We first derive a precise expression for $\mathcal{N}y$, that is useful in the proof of later results.

Lemma 2. *Let $G(y, r, \varepsilon) = G_0(y, r) + \varepsilon G_1(y, r) + O(\varepsilon^2)$, uniformly for (y, r) in some compact neighborhood of $\{(\overline{y}_0(r), r) \mid r \in H_0\}$. Then for $y \in \mathcal{B}(\varepsilon_0)$:*

$$\mathcal{N}y(r, \varepsilon) = \overline{y}_0(r) - \varepsilon L(r)^{-1} \cdot G_1(\overline{y}_0(r), r) + O(\varepsilon^2 + \|y - \overline{y}_0\|^2).$$

Proof. Considering the Taylor series of $G(y, r, \varepsilon)$ at $(\overline{y}_0(r), r, 0)$ we see that

$$G(y, r, \varepsilon) = G_0(\overline{y}_0(r), r) + D_y G_0(\overline{y}_0(r), r) \cdot (y - \overline{y}_0(r))$$
$$+ \varepsilon G_1(\overline{y}_0(r), r)) + O(\varepsilon^2 + \|y - \overline{y}_0\|^2).$$

Since $G_0(\overline{y}_0(r), r) = 0$ and $D_y G_0(\overline{y}_0(r), r) = L(r)$, it follows from the definition of $\mathcal{N}$ that

$$\mathcal{N}y(r, \varepsilon) = y(r, \varepsilon) - L(r)^{-1} \cdot L(r) \cdot (y(r, \varepsilon) - \overline{y}_0(r))$$
$$- \varepsilon L(r)^{-1} \cdot G_1(\overline{y}_0(r), r) + O(\varepsilon^2 + \|y - \overline{y}_0\|^2)$$
$$= \overline{y}_0(r) - \varepsilon L(r)^{-1} \cdot G_1(\overline{y}_0(r), r)) + O(\varepsilon^2 + \|y - \overline{y}_0\|^2).$$

This completes the proof of the lemma. $\qquad\qquad\qquad\qquad\qquad\qquad\qquad\qquad\square$

The preceding lemma shows that $\mathcal{N}y(r, \varepsilon)$ is of the form $\overline{y}_0(r) + O(\varepsilon)$, provided $y(r, \varepsilon) = \overline{y}_0(r) + O(\varepsilon)$. To make this observation more precise we introduce the space

$$\mathcal{B}(\varepsilon_0, \beta) = \{y : H_0 \times [-\varepsilon_0, \varepsilon_0] \to \mathbb{R}^d \mid \sup_{r \in H_0} |y(r, \varepsilon) - \overline{y}_0(r)| \le \beta\varepsilon\},$$

where ε_0 and β are positive constants; ε_0 is small, β is specified later. The space $\mathcal{B}(\varepsilon_0, \beta)$ is a closed subspace of $\mathcal{B}(\varepsilon_0)$, so in particular it is a complete metric space. The following properties of the Newton operator are crucial in the derivation of our algorithm.

Theorem 3. *Let β be a constant such that*

$$\beta > \sup_{r \in H_0} \|L(r)^{-1} \cdot G_1(\overline{y}_0(r), r)\|.$$

(i) *For small values of ε_0 the space $\mathcal{B}(\varepsilon_0, \beta)$ is $\mathcal{N}$–invariant, i.e.:*

$$\mathcal{N}(\mathcal{B}(\varepsilon_0, \beta)) \subset \mathcal{B}(\varepsilon_0, \beta).$$

(ii) *For small values of ε_0 the Newton operator $\mathcal{N}$ is a contraction on $\mathcal{B}(\varepsilon_0, \beta)$ with contraction factor $O(\varepsilon_0)$. Its fixed point $\overline{y}$ satisfies*

$$G(\overline{y}(r, \varepsilon), r, \varepsilon) = 0,$$

and is of the form $\overline{y}(r, \varepsilon) = \overline{y}_0(r) + \varepsilon\overline{y}_1(r) + O(\varepsilon^2)$, uniformly in $r \in H_0$, where

$$\overline{y}_1(r) = -L(r)^{-1} \cdot G_1(\overline{y}_0(r), r). \tag{10}$$

(iii) Let $\{y_n\} \subset \mathcal{B}(\varepsilon_0, \beta)$ be a sequence with $y_0 \in \mathcal{B}(\varepsilon_0, \beta)$, and $y_{n+1} = \mathcal{N} y_n$. Then, for all γ with $0 < \gamma < 1$, there is an $\varepsilon_0 > 0$ such that:

$$y_n(r, \varepsilon) = \overline{y}(r, \varepsilon) + O(\varepsilon^{\gamma n}),$$

uniformly for $|\varepsilon| \leq \varepsilon_0$ and $r \in H_0$, as $n \to \infty$.

Proof. (i) This is a straightforward consequence of lemma 2.

(ii) Let $y_1, y_2 \in \mathcal{B}(\varepsilon_0, \beta)$. To prove that $\mathcal{N}$ is a contraction, we Taylor–expand $G(y, r, \varepsilon)$ at $(y_1(r, \varepsilon), r, \varepsilon)$ to obtain:

$$G(y_2(r, \varepsilon), r, \varepsilon) = G(y_1(r, \varepsilon), r, \varepsilon) + D_y G(y_1(r, \varepsilon), r, \varepsilon) \cdot (y_2(r, \varepsilon) - y_1(r, \varepsilon))$$
$$+ O(|y_2(r, \varepsilon) - y_1(r, \varepsilon)|^2).$$

Since $D_y G(y_1(r, \varepsilon), r, \varepsilon) = L(r) + O(\varepsilon + |y_1(r, \varepsilon) - \overline{y}_0(r)|)$, we derive that

$$\mathcal{N} y_2(r, \varepsilon) - \mathcal{N} y_1(r, \varepsilon) = O(\varepsilon + |y_1(r, \varepsilon) - \overline{y}_0(r)|) \cdot (y_2(r, \varepsilon) - y_1(r, \varepsilon)) +$$
$$O(|y_2(r, \varepsilon) - y_1(r, \varepsilon)|^2).$$

Since $|y_1(r, \varepsilon) - \overline{y}_0(r)| \leq c\varepsilon$, and $|y_2(r, \varepsilon) - y_1(r, \varepsilon)| \leq 2c\varepsilon$, we see that

$$|\mathcal{N} y_2(r, \varepsilon) - \mathcal{N} y_1(r, \varepsilon)| = O(\varepsilon)|y_2(r, \varepsilon) - y_1(r, \varepsilon)|,$$

so $\|\mathcal{N} y_2 - \mathcal{N} y_1\| \leq O(\varepsilon_0)\|y_2 - y_1\|$. Hence $\mathcal{N}$ is a contraction, with contraction factor $O(\varepsilon_0)$.

Obviously $\mathcal{N}\overline{y} = \overline{y}$ is equivalent to $G(\overline{y}(r, \varepsilon), r, \varepsilon) = 0$. Furthermore lemma 2 yields $\overline{y}(r, \varepsilon) = \overline{y}_0(r) + \varepsilon\overline{y}_1(r) + O(\varepsilon^2)$.

(iii) We use induction with respect to n. Our inductive hypothesis for $n \geq 1$ is: $|y_n(r, \varepsilon) - \overline{y}(r, \varepsilon)| \leq \varepsilon^{\gamma n}$, for $r \in H_0$ and $|\varepsilon| \leq \varepsilon_0$. (We determine the constant $\varepsilon_0 > 0$ in the inductive step.) Observe that lemma 2 and part (ii) imply

$$\sup_{r \in H_0} |\overline{y}(r, \varepsilon) - y_n(r, \varepsilon)| = O(\varepsilon^2),$$

for all $n \geq 1$, we see that the inductive hypothesis holds for $n = 1, 2$. So assume it holds true for $n \geq 2$.

Using $G(\overline{y}(r, \varepsilon), r, \varepsilon) = 0$, we see that the Taylor expansion of G at $(\overline{y}(r, \varepsilon), r, \varepsilon)$ is of the form

$$G(y, r, \varepsilon) = D_y G(\overline{y}(r, \varepsilon), r, \varepsilon) \cdot (y - \overline{y}(r, \varepsilon)) + R(y, r, \varepsilon),$$

where the higher order term R satisfies

$$|R(y, r, \varepsilon)| \leq c_0 |y - \overline{y}(r, \varepsilon)|^2,$$

for some positive constant c_0, uniformly for (y, r, ε) ranging over some compact neighborhood of $\{\overline{y}_0(r), r, 0) \mid r \in H_0\}$ in $\mathbb{R}^d \times H_0 \times [-\varepsilon_0, \varepsilon_0]$.

Furthermore, $D_y G(\overline{y}(r, \varepsilon), r, \varepsilon)$ is of the form $L(r) + \Delta(r, \varepsilon)$, where $\|\Delta(r, \varepsilon)\| \leq c_1 \varepsilon$ for some positive constant c_1. Then

$$y_{n+1}(r, \varepsilon) - \overline{y}(r, \varepsilon) = -L(r)^{-1}(\Delta(r, \varepsilon) \cdot (y_n(r, \varepsilon) - \overline{y}(r, \varepsilon)) + R(y_n(r, \varepsilon), r, \varepsilon)).$$

Therefore

$$|y_{n+1}(r, \varepsilon) - \overline{y}(r, \varepsilon)| \leq \|L(r)^{-1}\|(c_1 \varepsilon^{\gamma n + 1} + c_0 \varepsilon^{2\gamma n})$$
$$= \varepsilon^{\gamma(n+1)} \|L(r)^{-1}\|(c_1 \varepsilon^{1-\gamma} + c_0 \varepsilon^{\gamma(n-1)}).$$

Therefore the inductive hypothesis holds for $n + 1$, provided we started out with a value of ε_0 satisfying

$$\sup_{r \in H_0} \|L(r)^{-1}\|(c_1 \varepsilon_0^{1-\gamma} + c_0 \varepsilon_0^\gamma) \leq 1.$$

$\square$

Theorem 3(ii) reveals that $y_1(r, \varepsilon) = \overline{y}_0(r) + \varepsilon \overline{y}_1(r)$ is a good initial guess for the solution of (8), and theorem 3(iii) guarantees that each application of the Newton operator $\mathcal{N}$ brings us closer to the fixed point roughly by a factor of $O(\varepsilon^\gamma)$. In the next section we apply these observations to the computation of the graph transform.

3.3. Computing the invariant manifold

In this section we apply the results of section 3.2 to compute the graph transform. To this end we first derive, in section 3.3.1, a more precise expression for equation (8), and apply our extension of Newton's method to solve it. It turns out that we can determine the image of the graph transform analytically up to terms of order ε^2, see section 3.3.2. This analysis enables us to iterate the graph transform starting from a good initial guess of the fixed point. A priori, the fixed point of the graph transform defines a C^0 invariant manifold $\mathbb{H}_\varepsilon$ of f_ε, for small values of ε. According to [10] it is even C^1. Although we can extend the analysis of this section to prove this stronger result as well, we abstain from doing so, since we are merely heading for an algorithm to compute the invariant manifold. In section 3.4 we present a method to compute the continuous Df_ε–invariant splitting of the tangent bundle of $\mathbb{H}_\varepsilon$.

We assume that (a representation of) the invariant splitting $\mathbb{T}_r(\mathbb{H}_0) \oplus \mathbb{N}_r^s(\mathbb{H}_0)$, the restrictions ϱ_0 and σ_0 of f_0^{-1} and f_0 to H_0, and the derivative $Df_0(r) = A_0(r) \oplus K_0(r)$ are given for all $r \in H_0$.

3.3.1. The Newton operator

First we transform equation (4) into an equation of the form (8). Ideally we like to find a function $G : \mathbb{R}^d \times H_0 \times \mathbb{R} \to \mathbb{R}^d$ such that $G_\varepsilon(y, r) = 0$ iff y is the point on graph(η_ε) above $r \in H_0$, where η_ε is the image of h_ε under the graph transform Γ_{f_ε}, see figure 2. In other words, $\eta_\varepsilon(r)$ is the second component of the solution $(\varrho_\varepsilon(r), \eta_\varepsilon(r))$ of equation ((4)). This could be achieved by designing a diffeomorphism $\psi_\varepsilon : H_0 \times \mathbb{R}^s \to \mathbb{R}^d$ such that $\psi_\varepsilon(\varrho_\varepsilon(r), \eta_\varepsilon(r)) = \Phi(r, \eta_\varepsilon(r))$, and by taking G such that $G_\varepsilon(\psi_\varepsilon(\xi, \eta), r) = F_\varepsilon(\xi, \eta, r)$. An obvious definition is $\psi_\varepsilon(\xi, \eta) = \Phi(\sigma_\varepsilon(\xi), \eta)$, with $\sigma_\varepsilon(\xi) = \sigma(\xi, \varepsilon)$ defined by ((7)). However, σ_ε is rather awkward to compute for $\varepsilon \neq 0$. In view of our assumption that (a representation of) σ_0 is given, we use ψ_0 instead of ψ_ε even for $\varepsilon \neq 0$, i.e. we consider the map $\Psi : H_0 \times \mathbb{R}^s \to \mathbb{R}^d$, defined by

$$\Psi(\xi, \eta) = \Phi(\sigma_0(\xi), \eta), \tag{11}$$

which is a diffeomorphism from a neighborhood of $H_0 \times \{0\}$ in $H_0 \times \mathbb{R}^s$ to a neighborhood of $\mathbb{H}_0$ in $\mathbb{R}^d$. Then define G by:

$$G(\Psi(\xi, \eta), r, \varepsilon) = F(\xi, \eta, r, \varepsilon). \tag{12}$$

Since $\varphi_0(r) = \Phi(r, 0) = \Psi(\varrho_0(r), 0)$, for $r \in H_0$, we see that $G(\varphi_0(r), r, 0) = F(\varrho_0(r), 0, r, 0) = 0$, so the first part of condition (9) is satisfied for $\overline{y}_0 = \varphi_0$. To check that the second part holds as well, we first derive an expression for $L(r) = D_y G(\varphi_0(r), r, 0) : \mathbb{R}^d \to \mathbb{R}^d$. It turns out that $L(r)$ has a very simple expression with respect to the splitting $\mathbb{T}_r(\mathbb{H}_0) \oplus \mathbb{N}_r^s(\mathbb{H}_0)$ on both its domain and its range. More precisely:

Lemma 4. *For $r \in H_0$, the splitting $\mathbb{R}^d = \mathbb{T}_r(\mathbb{H}_0) \oplus \mathbb{N}_r^s(\mathbb{H}_0)$ is $L(r)$–invariant, and for $v_c \in \mathbb{T}_r(\mathbb{H}_0)$, $v_s \in \mathbb{N}_r^s(\mathbb{H}_0)$*

$$L(r)(v_c \oplus v_s) = v_c \oplus (-v_s).$$

In particular $L(r)$ is invertible, and $L(r)^{-1} = L(r)$.

Proof. Recall that for $(\xi, \eta, r) \in H_0 \times \mathbb{R}^s \times H_0$:

$$F_0(\xi, \eta, r) = f_0(\Phi(\xi, 0)) - \Phi(r, \eta) = \Psi(\xi, 0) - \Psi(\varrho_0(r), \eta), \tag{13}$$

since $f_0(\Phi(\xi, 0)) = f_0(\varphi_0(\xi)) = \varphi_0(\sigma_0(\xi)) = \Psi(\xi, 0)$, and $\Phi(r, \eta) = \Phi(\sigma_0(\varrho_0(r)), \eta) = \Psi(\varrho_0(r), \eta)$. From (13) we derive

$$D_\xi F_0(\varrho_0(r), 0, r) = D_\xi \Psi(\varrho_0(r), 0),$$
$$D_\eta F_0(\varrho_0(r), 0, r) = -D_\eta \Psi(\varrho_0(r), 0).$$

Since

$$D_{(\xi,\eta)}F_0(\varrho_0(r),0,r) = D_y G_0(\varphi_0(r),r) \cdot D\Psi(\varrho_0(r),0) = L(r) \cdot D\Psi(\varrho_0(r),0),$$

the proof is complete. $\square$

Lemma 4 yields the following straightforward method of computing $\mathcal{N}y$ for $y \in \mathcal{B}(\varepsilon_0,\beta)$.

Algorithm   Newton
Input: $y : H_0 \times [-\varepsilon_0, \varepsilon_0] \to \mathbb{R}^d$.
Output: $\mathcal{N}y : H_0 \times [-\varepsilon_0, \varepsilon_0] \to \mathbb{R}^d$.
forall $r \in H_0, \varepsilon \in [-\varepsilon_0, \varepsilon_0]$ **do**
1                $x \leftarrow \pi_c(y(r,\varepsilon))$
                   Comment: $x \in H_0$ and $y(r,\varepsilon) - \varphi_0(x) \in \mathbb{N}_x^s(\mathbb{H}_0)$
2                $\eta \leftarrow \iota_x(y(r,\varepsilon) - \varphi_0(x))$
                   Comment: $y(r,\varepsilon) = \Phi(x,\eta)$
3                $Y \leftarrow F(\varrho_0(x),\eta,r,\varepsilon)$
                   Comment: $Y = G(y(r,\varepsilon),r,\varepsilon)$
4                $Y^c \leftarrow \Pi_r^c(Y)$
                   $Y^s \leftarrow \Pi_r^s(Y)$
5                $\mathcal{N}y(r,\varepsilon) \leftarrow y(r,\varepsilon) - Y^c + Y^s$
                   Comment: $L(r)^{-1} \cdot G(y(r,\varepsilon),r,\varepsilon) = Y^c - Y^s$

A few further comments are in order. Execution of line 1 amounts to finding the point $\varphi_0(x) \in \mathbb{H}_0$ such that $y(r,\varepsilon) \in \varphi_0(x) + \mathbb{N}_x^s(\mathbb{H}_0)$. The maps ι_x, Π_x^c, Π_x^s and F have straightforward implementations; see their definitions (3), (2) and (5), respectively. In section 6, where we discuss the discretization problem, we indicate how to find implementations that have a predescribed accuracy. Since also (a representation of) the map $\varrho_0 : H_0 \to H_0$ is given, lines 2, 3 and 4 can be implemented in a straightforward way. To justify the comment at line 3, observe that

$$\begin{aligned}
G(y(r,\varepsilon),r,\varepsilon) &= G(\Phi(x,\eta),r,\varepsilon) \\
&= G(\Psi(\varrho_0(x),\eta),r,\varepsilon) \\
&= F(\varrho_0(x),\eta,r,\varepsilon) \\
&= Y.
\end{aligned}$$

Finally the correctness of line 5 follows from lemma 4.

3.3.2. Using the graph transform to compute $\mathbb{H}_\varepsilon$

The map $\Psi : H_0 \times \mathbb{R}^s \to \mathbb{R}^d$, transforming F into G, also establishes a 1:1–correspondence between sections $\eta \in \Sigma(\varepsilon_0)$ and maps $y : H_0 \times \mathbb{R} \to \mathbb{R}^d$, defined

by $y(r, \varepsilon) = \Phi(r, \eta(r, \varepsilon))$. To apply the Newton operator, we should restrict the domain of the graph transform to sections, corresponding to maps in the domain $\mathcal{B}(\varepsilon_0, \beta)$ of the Newton operator. Therefore we consider the subset $\Sigma(\varepsilon_0, \alpha)$ of $\Sigma(\varepsilon_0)$, defined by

$$\Sigma(\varepsilon_0, \alpha) = \{h \in \Sigma(\varepsilon_0) \mid \sup_{r \in H_0} |h(r, \varepsilon)| \leq \alpha \varepsilon\}.$$

Since H_0 is compact, for $\beta > 0$ there is an $\alpha > 0$ such that a section in $\Sigma(\varepsilon_0, \alpha)$ corresponds to a map in $\mathcal{B}(\varepsilon_0, \beta)$. Hence, the image of a section $h \in \Sigma(\varepsilon_0, \alpha_0)$ under the graph transform Γ_f can be determined using algorithm NEWTON, designed in section 3.3.1. To obtain a good starting point for repeated application of the Newton operator, we first have to determine $G_1(\varphi_0(r), r) = \dfrac{\partial G}{\partial \varepsilon}(\varphi_0(r), r, 0)$, see theorem 3(ii), equation (10). To express G_1 in terms of the linear part of f and h, let

$$f(p, \varepsilon) = f_0(p) + \varepsilon f_1(p) + O(\varepsilon^2),$$

and

$$h(r, \varepsilon) = \varepsilon(h_1(r), \cdots, h_s(r)) + O(\varepsilon^2).$$

Lemma 5. *For $r \in H_0$*

$$G_1(\varphi_0(r), r) = \sum_{i,j=1}^{s} h_i(\varrho_0(r)) \kappa_{ij}(\varrho_0(r)) v_j^s(r) + f_1(\varphi_0(\varrho_0(r))).$$

Proof. Let $(y, r) \in \mathbb{R}^d \times H_0$, then $G_1(y, r) = \dfrac{\partial G}{\partial \varepsilon}(y, r, 0)$. Furthermore, let $y = \Psi(\xi_0, \eta_0)$, for $(\xi_0, \eta_0) \in H_0 \times \mathbb{R}^s)$, with Ψ as in (11), i.e.

$$y = \Phi(\sigma_0(\xi_0), \eta_0),$$

then $G(y, r, \varepsilon) = F(\xi_0, \eta_0, r, \varepsilon)$. Therefore,

$$G(y, r, \varepsilon) = f(p(\varepsilon), \varepsilon) - \Phi(r, \eta_0),$$

where $p(\varepsilon) = \Phi(\xi_0, \varepsilon h(\xi_0, \varepsilon))$. In particular $p_0 := p(0) = \varphi_0(\xi_0)$. Hence,

$$G_1(y, r) = Df_0(p_0) \cdot \dot{p}(0) + f_1(p_0),$$

with

$$\dot{p}(0) = \sum_{i=1}^{s} h_i(\xi_0) v_i^s(\xi_0).$$

Therefore,

$$G_1(y, r) = Df_0(p_0) \cdot \left(\sum_{i=1}^{s} h_i(\xi_0) v_i^s(\xi_0) \right) + f_1(p_0)$$

$$= \sum_{i,j=1}^{s} h_i(\xi_0) \kappa_{ij}(\xi_0) v_j^s(\sigma_0(\xi_0)) + f_1(p_0).$$

We obtain the desired expression by substituting $y = \varphi_0(r)$, in which case $\sigma_0(\xi_0) = r$ and hence $\xi_0 = \varrho_0(r)$. $\qquad\square$

For $p = \varphi_0(r)$, with $r \in H_0$, the curve $\varepsilon \mapsto f(\varphi_0(r), \varepsilon)$ passes through $f_0(\varphi_0(r)) = \varphi_0(\sigma_0(r))$. Therefore its tangent vector at this point, viz $f_1(\varphi_0(r))$, belongs to $T_{\varphi_0(\sigma_0(r))}(\mathbb{R}^d)$, which we identify with $\mathbb{T}_{\sigma_0(r)}(\mathbb{H}_0) \oplus \mathbb{N}^s_{\sigma_0(r)}(\mathbb{H}_0)$. Therefore there are unique C^0 functions $V^c, V^s \to \mathbb{R}^d$, with $V^c(r) \in \mathbb{T}_r(\mathbb{H}_0)$ and $V^s(r) \in \mathbb{N}^s_r(\mathbb{H}_0)$, such that $f_1(\varphi_0(r)) = V^c(\sigma_0(r)) + V^s(\sigma(r))$. Since ϱ_0 is the inverse of σ_0, we see that $f_1(\varphi_0(\varrho_0(r))) = V^c(r) + V^s(r)$, in other words:

$$V^c(r) = \Pi^c_r(f_1(\varphi_0(\varrho_0(r)))) \quad \text{and} \quad V^s(r) = \Pi^s_r(f_1(\varphi_0(\varrho_0(r)))).$$

Corollary 6. *The fixed point $\overline{y}$ of $\mathcal{N}$ is of the form $\overline{y}(r, \varepsilon) = \varphi_0(r) + \varepsilon \overline{y}_1(r) + O(\varepsilon^2)$, where*

$$\overline{y}_1(r) = \sum_{i,j=1}^{s} h_i(\varrho_0(r)) \kappa_{ij}(\varrho_0(r)) v_j^s(r) - V^c(r) + V^s(r) \qquad (14)$$

Algorithm   GRAPH TRANSFORM
Input: $h \in \Sigma(\varepsilon_0, \alpha)$, $\delta > 0$ (maximal error)
Output: $\Gamma_f(h) \in \Sigma(\varepsilon_0, \alpha)$
forall $r \in H_0, \varepsilon \in [-\varepsilon_0, \varepsilon_0]$ **do**
1          $y(r, \varepsilon) \leftarrow \varphi_0(r) + \varepsilon \overline{y}_1(r)$
          Comment: cf corollary 6
2   **repeat**
3           $y_{\text{new}} \leftarrow \mathcal{N}y$
          Comment: Use algorithm NEWTON
4           $error \leftarrow \|y - y_{\text{new}}\|$
5           $y \leftarrow y_{\text{new}}$
6   **until** $error \leq \delta$
7        $\Gamma_f(h)(r, \varepsilon) \leftarrow \pi_s(y)$
          Comment: $\pi_s(y) = \pi_s(\Psi^{-1}(y))$

Remark 7. To compute $\overline{y}_1(r)$ in line 1 we use expression (14). In view of lemma 2 the variable y in algorithm GRAPH TRANSFORM satisfies the invariant $y = \varphi_0(r) +$

$\varepsilon \overline{y}_1(r) + O(\varepsilon^2)$. In particular the output $\Gamma_f(h)$ is of the form

$$\Gamma_f(h)(r, \varepsilon) = \varepsilon(\overline{h}_1(r), \cdots, \overline{h}_s(r)) + O(\varepsilon^2),$$

where $(\overline{h}_1(r), \cdots, \overline{h}_s(r)) = \pi_s(\overline{y}_1(r))$, i.e.

$$\sum_{i=1}^{s} \overline{h}_i(r) v_i^s(r) = \sum_{i,j=1}^{s} h_i(\varrho_0(r)) \kappa_{ij}(\varrho_0(r)) v_j^s(r) + V^s(r). \tag{15}$$

This enables us to initialize $y(r, \varepsilon)$ properly upon repeated application of the graph transform Γ_f. In fact, we can even compute the fixed point of Γ_f up to terms of order ε^2 by repeated application of (15).

The crucial properties of the graph transform Γ_f are reflected by the following theorem.

Theorem 8. *For any constant $\overline{\lambda}$, such that $\lambda < \overline{\lambda} < 1$, there are values of α and ε_0 such that:*
(i) Γ_f leaves $\Sigma(\varepsilon_0, \alpha)$ invariant, i.e.

$$\Gamma_f(\Sigma(\varepsilon_0, \alpha)) \subset \Sigma(\varepsilon_0, \alpha).$$

(ii) Γ_f is a contraction on $\Sigma(\varepsilon_0, \alpha)$, whose contraction factor does not exceed $\overline{\lambda}$.
(iii) The fixed point $\overline{h}$ of Γ_f defines a continuous family of C^1 embeddings $\varphi_\varepsilon :$ $H_0 \times [-\varepsilon_0, \varepsilon_0] \to \mathbb{R}^d$ by $\varphi_\varepsilon(r) = \Phi(r, \overline{h}_\varepsilon(r))$, such that $\mathbb{H}_\varepsilon := \varphi_\varepsilon(H_0)$ is the 1–normally hyperbolic invariant manifold of f_ε.

Proof. (i) The first property is in fact equivalent to theorem 3 (i). Let C be a constant such that $\sup_{r \in H_0} \|V^s(r)\| < C$. In view of the expression for $\Gamma_f(h)$, derived in remark 7, we see that

$$|\Gamma_f(h)(r, \varepsilon)| \le \varepsilon(\lambda|h(r, \varepsilon)| + C) + O(\varepsilon).$$

Taking α such that $\lambda \alpha + C < \alpha$, and taking ε_0 sufficiently small, we see that $\Sigma(\varepsilon_0, \alpha)$ is Γ_f–invariant.
    (ii) Note that (15) implies that for $h_1, h_2 \in \Sigma(\varepsilon_0, \alpha)$:

$$\|\Gamma_f(h_2) - \Gamma_f(h_1)\| \le \overline{\lambda}\|h_2 - h_1\|,$$

provided ε_0 is sufficiently small. This proves that Γ_f is a contraction.
    (iii) Note that (i) and (ii) only guarantee that the fixed point $\overline{h}$ is a *continuous* section. Therefore, the map φ_ε is a C^0 embedding, and the set $\mathbb{H}_\varepsilon = \varphi_\varepsilon(H_0)$ is a C^0 invariant manifold for f_ε. We can even prove, with the machinery of the next subsection, that $\mathbb{H}_\varepsilon$ is a C^1 manifold. We postpone completion of this part of the proof to the next subsection, viz to the proof of theorem 10. $\square$

3.4. Computing the invariant splitting of the tangent bundle

In the previous subsection we derived an algorithm that computes the invariant manifold $\mathbb{H}_\varepsilon \subset \mathbb{R}^d$ of f_ε as the image of an embedding $\varphi_\varepsilon : H_0 \to \mathbb{R}^d$. This algorithm computes a pair $(\overline{\varrho}, \overline{h})$, with $\overline{\varrho} : H_0 \times \mathbb{R} \to H_0$ and $\overline{h} : H_0 \times \mathbb{R} \to \mathbb{R}^s$, such that $\varphi_\varepsilon(r) = \Phi(r, \overline{h}_\varepsilon(r))$, and

$$f_\varepsilon(\varphi_\varepsilon(\overline{\varrho}_\varepsilon(r))) = \varphi_\varepsilon(r).$$

The inverse of $\overline{\varrho}_\varepsilon$ is denoted by $\overline{\sigma}_\varepsilon(r)$. Therefore

$$f_\varepsilon(\varphi_\varepsilon(r)) = \varphi_\varepsilon(\overline{\sigma}_\varepsilon(r)).$$

Hence

$$\overline{\sigma}_\varepsilon(r) = \pi_c f_\varepsilon(\varphi_\varepsilon(r)),$$

so $\overline{\sigma}_\varepsilon$ can easily be computed from φ_ε.

Our goal in this section is to compute the Df_ε–invariant splitting $T(\mathbb{H}_\varepsilon) \oplus \mathbb{N}^s(\mathbb{H}_\varepsilon)$ of the tangent bundle $T_{\mathbb{H}_\varepsilon}(\mathbb{R}^d)$. To this end we write the map $Df_\varepsilon(\varphi_\varepsilon(r))$ with respect to the splittings $\mathbb{T}_r(\mathbb{H}_0) \oplus \mathbb{N}^s_r(\mathbb{H}_0)$ and $\mathbb{T}_{\overline{\sigma}_\varepsilon(r)}(\mathbb{H}_0) \oplus \mathbb{N}^s_{\overline{\sigma}_\varepsilon(r)}(\mathbb{H}_0)$ as

$$\begin{pmatrix} A_\varepsilon(r) & B_\varepsilon(r) \\ C_\varepsilon(r) & K_\varepsilon(r) \end{pmatrix},$$

where $A_\varepsilon(r) : \mathbb{T}_r(\mathbb{H}_0) \to \mathbb{T}_{\overline{\sigma}_\varepsilon(r)}(\mathbb{H}_0)$, $B_\varepsilon(r) : \mathbb{N}^s_r(\mathbb{H}_0) \to \mathbb{T}_{\overline{\sigma}_\varepsilon(r)}(\mathbb{H}_0)$, $C_\varepsilon(r) : \mathbb{T}_r(\mathbb{H}_0) \to \mathbb{N}^s_{\overline{\sigma}_\varepsilon(r)}(\mathbb{H}_0)$ and $K_\varepsilon(r) : \mathbb{N}^s_r(\mathbb{H}_0) \to \mathbb{N}^s_{\overline{\sigma}_\varepsilon(r)}(\mathbb{H}_0)$ are linear maps, depending continously on (r, ε). Note in particular that $B_0(r) = 0$ and $C_0(r) = 0$, and $\|A_\varepsilon(r)\| = \|A_0(r)\| + O(\varepsilon)$, etc.

The algorithm that computes the Df_ε–invariant splitting of $T_{\mathbb{H}_\varepsilon}(\mathbb{R}^d)$ is again based on a graph transform. Consider, for $(r, \varepsilon) \in H_0 \times \mathbb{R}$, linear maps $\omega_\varepsilon(r) : \mathbb{N}^s_r(\mathbb{H}_0) \to \mathbb{T}_r(\mathbb{H}_0)$, depending continously on (r, ε). The space of all such maps, defined for $(r, \varepsilon) \in H_0 \times [-\varepsilon_0, \varepsilon_0]$, is denoted by $\Omega_s(\varepsilon_0)$. It is a Banach space with norm defined by $\|\omega\| = \sup_{|\varepsilon| \le \varepsilon_0, r \in H_0} \|\omega_\varepsilon(r)\|$. Let $\Omega_s(\delta_0, \varepsilon_0)$ be the subspace consisting of those $\omega \in \Omega_s(\varepsilon_0)$ for which $\|\omega\| \le \delta_0$. Note that this is a closed subspace of $\Omega_s(\varepsilon_0)$, and therefore it is a complete metric space.

The graph of $\omega_\varepsilon(r)$ is the subspace $\mathrm{graph}(\omega_\varepsilon(r))$ of $\mathbb{R}^d$, defined by

$$\mathrm{graph}(\omega_\varepsilon(r)) = \{\omega_\varepsilon(r) \cdot u \oplus u \mid u \in \mathbb{N}^s_r(\mathbb{H}_0)\}.$$

We define the operator $\mathcal{T}_s$ on $\Omega_s(\delta_0, \varepsilon_0)$ by the requirement that, for $\overline{\omega} = \mathcal{T}_s(\omega)$,

$$\mathrm{graph}(\overline{\omega}_\varepsilon(r)) = Df_\varepsilon(\varphi_\varepsilon(r))^{-1} \mathrm{graph}(\omega_\varepsilon(\overline{\sigma}_\varepsilon(r))). \tag{16}$$

Then (16) boils down to: for all $v \in \mathbb{N}^s_{\overline{\sigma}_\varepsilon(r)}(\mathbb{H}_0)$ there is a $\overline{v} \in \mathbb{N}^s_r(\mathbb{H}_0)$ such that

$$\begin{pmatrix} \overline{\omega} \cdot \overline{v} \\ \overline{v} \end{pmatrix} = \begin{pmatrix} A & B \\ C & K \end{pmatrix}^{-1} \cdot \begin{pmatrix} \omega \cdot v \\ v \end{pmatrix},$$

where $A = A_\varepsilon(r)$ (etc.), $\overline{\omega} = \overline{\omega}_\varepsilon(r)$ and $\omega = \omega_\varepsilon(\overline{\sigma}_\varepsilon(r))$. Eliminating v and $\overline{v}$ we see that

$$\overline{\omega} = (A - \omega \cdot C)^{-1} \cdot (-B + \omega \cdot K),$$

in other words

$$(\mathcal{T}_s\omega)_\varepsilon(r) = (A_\varepsilon(r) - \omega_\varepsilon(\overline{\sigma}_\varepsilon(r)) \cdot C_\varepsilon(r))^{-1} \cdot (-B_\varepsilon(r) + \omega_\varepsilon(\overline{\sigma}_\varepsilon(r)) \cdot K_\varepsilon(r)). \quad (17)$$

Theorem 9. *Let $\overline{\lambda}$ and $\overline{\mu}$ be constants such that $\lambda < \overline{\lambda} < 1$ and $\mu < \overline{\mu} < 1$. Then, for δ_0 and ε_0 sufficiently small:*

(i) The space $\Omega_s(\delta_0, \varepsilon_0)$ is $\mathcal{T}_s$–invariant, i.e.

$$\mathcal{T}_s(\Omega_s(\delta_0, \varepsilon_0)) \subset \Omega_s(\delta_0, \varepsilon_0).$$

(ii) The operator $\mathcal{T}_s$ is a contraction, whose contraction factor does not exceed $\overline{\mu}$. Its fixed point $\overline{\omega}$ determines a Df_ε–invariant family $\{\mathbb{N}_r^s(\mathbb{H}_\varepsilon)\}_{r \in H_0}$ of subspaces of $\mathbb{R}^d$, defined by

$$\mathbb{N}_r^s(\mathbb{H}_\varepsilon) = graph(\overline{\omega}_\varepsilon(r)).$$

(iii) For $r \in H_0$ and $v \in \mathbb{N}_r^s(\mathbb{H}_\varepsilon)$:

$$\|Df_\varepsilon(\varphi_\varepsilon(r)) \cdot v\| \le \overline{\lambda}\|v\|.$$

Proof. (i) For $r \in H_0$ and $|\varepsilon| \le \varepsilon_0$:

$$\|(A_\varepsilon(r) - \omega_\varepsilon(r) \cdot C_\varepsilon(r))^{-1}\| \le \|A_\varepsilon(r)^{-1}\| + O(\varepsilon_0\|\omega_\varepsilon(r)\|),$$

and

$$\| - B_\varepsilon(r) + \omega_\varepsilon(r) \cdot K_\varepsilon(r)\| = O(\varepsilon_0) + \|\omega_\varepsilon(r)\|\|K_\varepsilon(r)\|.$$

Therefore

$$\begin{aligned}
\|\mathcal{T}_s\omega_\varepsilon(r)\| &\le \|A_\varepsilon(r)^{-1}\|\|\omega_\varepsilon(r)\|\|K_\varepsilon(r)\| + O(\varepsilon_0 + \|\omega\|^2) \\
&\le \mu\delta_0 + O(\varepsilon_0 + \|\omega\|^2) \\
&\le \delta_0,
\end{aligned}$$

for δ_0 and ε_0 sufficiently small.

(ii) Let $\omega_1, \omega_2 \in \Omega_s(\delta_0, \varepsilon_0)$. Writing again A instead of $A_\varepsilon(r)$, etc., we see that $\mathcal{T}_s$ is a contraction:

$$\begin{aligned}
\|\mathcal{T}_s\omega_2 - \mathcal{T}_s\omega_1\| \le &\|(A - \omega_2 \cdot C)^{-1} \cdot ((-B + \omega_2 \cdot K) - (-B + \omega_1 \cdot K))\| + \\
&\|((A - \omega_2 \cdot C)^{-1} - (A - \omega_1 \cdot C)^{-1}) \cdot (-B + \omega_1 \cdot K)\|
\end{aligned}$$

$$\leq \|(A - \omega_2 \cdot C)^{-1} \cdot (\omega_2 - \omega_1) \cdot K\| +$$
$$\|(A - \omega_2 \cdot C)^{-1} \cdot (\omega_1 - \omega_2) \cdot (A - \omega_1 \cdot C)^{-1}(-B + \omega_1 \cdot K)\|$$
$$\leq (\|A^{-1}\|\|K\|(1 + O(\delta_0 + \varepsilon_0)) + \|A^{-1}\|^2 O(\delta_0 + \varepsilon_0))\|\omega_1 - \omega_2\|$$
$$\leq (\mu + O(\delta_0 + \varepsilon_0))\|\omega_1 - \omega_2\|$$
$$\leq \overline{\mu}\|\omega_1 - \omega_2\|,$$

for δ_0 and ε_0 sufficiently small. (To derive the second inequality we use the identity $S_2^{-1} - S_1^{-1} = S_2^{-1} \cdot (S_1 - S_2) \cdot S_1^{-1}$.) Hence $\mathcal{T}_s$ is a contraction, whose contraction factor does not exceed $\overline{\mu}$.

(iii) Let $v \in \mathbb{N}_r^s(\mathbb{H}_\varepsilon)$, then $v = \overline{\omega}_\varepsilon(r) \cdot u \oplus u$, for some $u \in \mathbb{N}_r^s(\mathbb{H}_0)$. Since $\overline{\omega}$ is a fixed point of $\mathcal{T}_s$ it follows from (17) that $Df_\varepsilon(\varphi_\varepsilon(r)) \cdot v = \overline{\omega}(\overline{\sigma}_\varepsilon(r)) \cdot w \oplus w$, where $w = (C_\varepsilon(r) \cdot \overline{\omega}_\varepsilon(r) + K_\varepsilon(r)) \cdot u$. Hence

$$\|Df_\varepsilon(\varphi_\varepsilon(r)) \cdot v\| \leq (\|K_\varepsilon(r)\| + O(\|\overline{\omega}_\varepsilon(r)\|))\|u\|$$
$$\leq (\lambda + O(\delta_0 + \varepsilon_0))\|v\|$$
$$\leq \overline{\lambda}\|v\|,$$

for δ_0 and ε_0 sufficiently small. This completes the proof of the theorem. $\qquad\square$

To determine the tangent space of the invariant manifold $\mathbb{H}_\varepsilon$ of f_ε, we similarly introduce the space $\Omega_c(\varepsilon_0)$, consisting of families of linear maps $\omega_\varepsilon(r) : \mathbb{T}_r(\mathbb{H}_0) \to \mathbb{N}_r^s(\mathbb{H}_0)$, depending continuously on $(r, \varepsilon) \in H_0 \times \mathbb{R}$. Its subspace $\Omega_c(\delta_0, \varepsilon_0)$ consists of those $\omega \in \Omega_c(\varepsilon_0)$ with $\|\omega\| \leq \delta_0$. The operator $\mathcal{T}_c : \Omega_c(\varepsilon_0) \to \Omega_c(\varepsilon_0)$ is defined by the condition that $Df_\varepsilon(\varphi_\varepsilon(\overline{\varrho}_\varepsilon(r)))$ maps the graph of $\omega_\varepsilon(\overline{\varrho}_\varepsilon(r)$ onto the graph of $\omega_\varepsilon(r)$. More precisely,

$$\begin{pmatrix} \overline{v} \\ \overline{\omega} \cdot \overline{v} \end{pmatrix} = \begin{pmatrix} A & B \\ C & K \end{pmatrix} \cdot \begin{pmatrix} v \\ \omega \cdot v \end{pmatrix},$$

where $A = A_\varepsilon(\overline{\varrho}_\varepsilon(r)$ (etc.), $\omega = \omega_\varepsilon(\overline{\varrho}_\varepsilon(r))$ and $\overline{\omega} = \overline{\omega}_\varepsilon(r)$. Elimination of v and $\overline{v}$ yields the following expression for $\mathcal{T}_c$:

$$(\mathcal{T}_c\omega)_\varepsilon(r) = (C_\varepsilon(\overline{\varrho}_\varepsilon(r)) + K_\varepsilon(\overline{\varrho}_\varepsilon(r)) \cdot \omega_\varepsilon(\overline{\varrho}_\varepsilon(r)) \cdot$$
$$(A_\varepsilon(\overline{\varrho}_\varepsilon(r)) + B_\varepsilon(\overline{\varrho}_\varepsilon(r)) \cdot \omega_\varepsilon(\overline{\varrho}_\varepsilon(r)))^{-1}.$$

The following result is similar to theorem 9.

Theorem 10. *Let $\overline{\lambda}$ and $\overline{\mu}$ be constants such that $\lambda < \overline{\lambda} < 1$ and $\mu < \overline{\mu} < 1$. Then, for δ_0 and ε_0 sufficiently small:*
(i) The space $\Omega_c(\delta_0, \varepsilon_0)$ is $\mathcal{T}_c$–invariant, i.e.

$$\mathcal{T}_c(\Omega_c(\delta_0, \varepsilon_0)) \subset \Omega_c(\delta_0, \varepsilon_0).$$

(ii) *The operator $\mathcal{T}_c$ is a contraction, whose contraction factor does not exceed $\overline{\mu}$. Its fixed point $\overline{\varpi}$ defines the tangent bundle of $\mathbb{H}_\varepsilon$, i.e.*

$$\mathbb{T}_r(\mathbb{H}_\varepsilon) = \{u \oplus \overline{\varpi}(r) \cdot u \mid u \in \mathbb{T}_r(\mathbb{H}_0)\}.$$

(iii) *For $r \in H_0$, let $\overline{A}_\varepsilon(r) \oplus \overline{K}_\varepsilon(r)$ be the expression for $Df_\varepsilon(\varphi_\varepsilon(r))$ with respect to the Df_ε–invariant splitting $\mathbb{T}_r(\mathbb{H}_\varepsilon) \oplus \mathbb{N}_r^s(\mathbb{H}_\varepsilon)$ and $\mathbb{T}_{\overline{\sigma}_\varepsilon(r)}(\mathbb{H}_\varepsilon) \oplus \mathbb{N}_{\overline{\sigma}_\varepsilon(r)}^s(\mathbb{H}_\varepsilon)$ on domain and range. Then*

$$\|(\overline{A}_\varepsilon(r))^{-1}\| \|\overline{K}_\varepsilon(r)\| \leq \overline{\mu}.$$

In other words: $\mathbb{H}_\varepsilon$ is a 1–normally hyperbolic invariant manifold of f_ε.

Proof. Arguing as in the proof of theorem 9 we can prove that $\mathcal{T}_c$ (i) leaves $\Omega_c(\delta_0, \varepsilon_0)$ invariant, and (ii) is a contraction on this space, for sufficiently small δ_0 and ε_0. The proof of part (iii) is again similar to the proof of theorem 9. $\square$

Theorem 10 enables us to complete the proof of theorem 8. We have already seen that the fixed point φ_ε of the graph transform is continuous. However, with a little more work we can even establish a similar result if we restrict the domain of the graph transform to Lipschitz–sections; see [10] or [17] for details. This fact, viz that φ_ε is *Lipschitz*, together with the observation that the family of spaces $\mathrm{graph}(\overline{\varpi}_\varepsilon(r))$, $r \in H_0$, is Df_ε–invariant, implies that $\mathrm{graph}(\overline{\varpi}_\varepsilon(r))$ is tangent to $\mathbb{H}_\varepsilon$ at $\varphi_\varepsilon(r)$, for all $r \in H_0$. Therefore φ_ε is a C^1 embedding, whose image $\mathbb{H}_\varepsilon$ is therefore C^1 as well.

3.5. Continuation

In many examples one may want to compute a continuous family of invariant manifolds for a family f_ε of diffeomorphisms, where ε ranges over a parameter interval that is not necessarily small. To apply the algorithm to such *continuation problems* we increase the parameter in small steps (possibly adapting the step size near parameter values for which the normal hyperbolicity is weak), and adjust the invariant splitting after each increase of the parameter ε. In this setting the algorithm has to deliver output, that serves as input to the next step in the continuation process, viz the increase of the parameter ε. The input to the algorithm, that computes the invariant manifold, has been described at the beginning of section 3.3. In view of the condition that the output of the algorithm has to be of the same type as the input, we therefore require that for a certain value of ε the algorithm computes:

- An embedding $\varphi_\varepsilon : H_0 \to \mathbb{R}^d$, whose image is the invariant manifold $\mathbb{H}_\varepsilon$ of f_ε. This embedding is computed by repeated application of algorithm GRAPH TRANSFORM; see section 3.3.2.

- A diffeomorphism $\overline{\varrho}_\varepsilon : H_0 \to H_0$, together with its inverse $\overline{\sigma}_\varepsilon$, such that $f_\varepsilon(\varphi_\varepsilon(\overline{\varrho}_\varepsilon(r))) = \varphi_\varepsilon(r)$ (as we have seen, $\overline{\varrho}_\varepsilon$ may be considered as the restriction of f_ε^{-1} to $\mathbb{H}_\varepsilon$). In fact, repeated application of algorithm GRAPH TRANSFORM not only yields the embedding φ_ε, but also the map $\overline{\varrho}_\varepsilon$; see again section 3.3.2.

- The Df_ε–invariant splitting $\mathbb{T}(\mathbb{H}_\varepsilon) \oplus \mathbb{N}^s(\mathbb{H}_\varepsilon)$ of the tangent bundle $T_{\mathbb{H}_\varepsilon}(\mathbb{R}^d)$. In particular, we assume that $\mathbb{N}_r^s(\mathbb{H}_\varepsilon)$ is represented by the vectors $v_i^s(r, \varepsilon) \in \mathbb{R}^d$, $1 \leq i \leq s$, which define an orthonormal system with respect to the Riemannian metric on $\mathbb{R}^d$. The computation of this splitting is described in section 3.4.

Hence the algorithm can be applied without further adaptations to the computation of invariant manifolds in a continuation setting. We illustrate our method with several examples in section 7.

4. Special case II: absence of normal contraction

In this section we develop an algorithm for the computation of the invariant manifold in the special case of absence of normal contraction, viz $N^s(H_0) = 0$. Here we drop the superscript u from our notation, by writing e.g. $K_0(r)$, $\kappa_{ij}(r)$, instead of $K_0^u(r)$, $\kappa_{ij}^u(r)$, etc.

Again we define the graph transform $h \mapsto \eta$ by requiring that f_ε^{-1} maps a point of the form $\Phi(\sigma, h(\sigma, \varepsilon))$ onto a point of the form $\Phi(r, \eta)$. In other words: η is the second component of the solution $(\sigma(r, \varepsilon), \eta(r, \varepsilon))$ of the equation

$$f_\varepsilon^{-1}(\Phi(\sigma, h(\sigma, \varepsilon))) = \Phi(r, \eta). \tag{18}$$

This leads to a version of the algorithm that is completely similar to that of section 3.3, with the understanding that f_ε is replaced with f_ε^{-1}.

From an algorithmic point of view the computation of f_ε^{-1} may degrade the performance dramatically. So we briefly describe an alternative approach, in which the graph transform is obtained by solving the equation

$$F(\sigma, \eta, r, \varepsilon) = 0, \tag{19}$$

where $F : H_0 \times \mathbb{R}^u \times H_0 \times \mathbb{R} \to \mathbb{R}^d$ is defined by

$$F(\sigma, \eta, r, \varepsilon) = f(\Phi(r, \eta), \varepsilon) - \Phi(\sigma, h(\sigma(r, \varepsilon), \varepsilon)). \tag{20}$$

This equation is equivalent to (18), but releaves us from the burden of computing f_ε^{-1} in the evaluation of F. Note that $F(\sigma_0(r), 0, r, 0) = f_0(\varphi_0(r)) - \varphi_0(\sigma_0(r)) = 0$. Therefore, in this case we define $G : \mathbb{R}^d \times H_0 \times \mathbb{R} \to \mathbb{R}^d$ by

$$G(\Psi(\xi, \eta), r, \varepsilon) = F(\xi, \eta, r, \varepsilon), \tag{21}$$

with $\Psi : H_0 \times \mathbb{R}^s \to \mathbb{R}^d$ defined by

$$\Psi(\xi, \eta) = \Phi(\varrho_0(\xi), \eta). \tag{22}$$

Note that, since $\varphi_0(r) = \Psi(\sigma_0(r), 0)$, we have $G(\varphi_0(r), r, 0) = 0$.

As in lemma 4 the linear map $L(r) = D_y G(\varphi_0(r), r, 0)$ has a simple expression, that is convenient for the implementation of our algorithm if there is no normal contraction.

Lemma 11. *The linear map*

$$L(r) : \mathbb{N}_r^u(\mathbb{H}_0) \oplus \mathbb{T}_r(\mathbb{H}_0) \to \mathbb{N}_{\sigma_0(r)}^u(\mathbb{H}_0) \oplus \mathbb{T}_{\sigma_0(r)}(\mathbb{H}_0)$$

leaves the direct sum composition invariant, and for $v_c \in \mathbb{T}_r(\mathbb{H}_0)$, $v_u \in \mathbb{N}_r^u(\mathbb{H}_0)$

$$L(r)(v_u \oplus v_c) = K_0(r)v_u \oplus (-A_0(r)v_c).$$

In particular, $L(r)$ is invertible, and $L(r)^{-1} = K_0(r)^{-1} \oplus (-A_0(r)^{-1})$.

Proof. Taking $\varepsilon = 0$ in (20) we see that:

$$\begin{aligned} F_0(\xi, \eta, r) &= f_0(\Phi(r, \eta)) - \Phi(\xi, 0) \\ &= f_0(\Phi(r, \eta)) - \varphi_0(\xi). \end{aligned}$$

Therefore

$$D_\xi F_0(\sigma_0(r), 0, r) = -D\varphi_0(\sigma_0(r)), \tag{23}$$
$$D_\eta F_0(\sigma_0(r), 0, r) = Df_0(\varphi_0(r)) \cdot D_\eta \Phi(r, 0). \tag{24}$$

Since $L(r) = D_y G_0(\varphi_0(r), r)$, and $F_0(\xi, \eta, r) = G_0(\Psi(\xi, \eta), r)$, we see that

$$\begin{aligned} D_\xi F_0(\sigma_0(r), 0, r) &= L(r) \cdot D_\xi \Psi(\sigma_0(r), 0) \\ &= L(r) \cdot D_\xi \Phi(r, 0) \cdot D\varrho_0(\sigma_0(r)) \\ &= L(r) \cdot D\varphi_0(r) \cdot D\varrho_0(\sigma_0(r)). \end{aligned} \tag{25}$$

On the other hand we have $\varphi_0(r) = f_0(\varphi_0(\varrho_0(r)))$, so

$$D\varphi_0(\sigma_0(r)) = Df_0(\varphi_0(r)) \cdot D\varphi_0(r) \cdot D\varrho_0(\sigma_0(r)). \tag{26}$$

Since $D\varphi_0(r) \cdot D\varrho_0(\sigma_0(r))$ is an isomorphism $T_{\sigma_0(r)}(H_0) \to \mathbb{T}_r(\mathbb{H}_0)$, we derive from (23), (25) and (26) that

$$L(r) \mid \mathbb{T}_r(\mathbb{H}_0) = -Df_0(\varphi_0(r)) \mid \mathbb{T}_r(\mathbb{H}_0).$$

Using (24) we conclude similarly

$$L(r) \mid \mathbb{N}_r^u(\mathbb{H}_0) = Df_0(\varphi_0(r)) \mid \mathbb{N}_r^u(\mathbb{H}_0).$$

Since $Df_0(\varphi_0(r)) \mid \mathbb{T}_r(\mathbb{H}_0) = A_0(r)$ and $Df_0(\varphi_0(r)) \mid \mathbb{N}_r^u(\mathbb{H}_0) = K_0(r)$, this completes the proof. $\qquad\qquad\qquad\qquad\qquad\qquad\qquad\qquad\qquad\qquad\qquad\qquad\qquad\square$

Suppose that $h\colon H_0 \to \mathbb{R}^u$ is of the form:

$$h(r, \varepsilon) = \varepsilon(h_1(r), \cdots, h_u(r)) + O(\varepsilon^2). \qquad\qquad (27)$$

The expression for G_1 in this case is (cf lemma 5):

Lemma 12. *For $r \in H_0$:*

$$G_1(\varphi_0(r), r) = f_1(\varphi_0(r)) - \sum_{i=1}^{u} h_i(\sigma_0(r))v_i^u(\sigma_0(r)). \qquad\qquad (28)$$

Proof. For $y \in \mathbb{R}^d$ we have $G(y, r, \varepsilon) = F(\xi, \eta, r, \varepsilon)$, where $(\xi, \eta) = \Psi^{-1}(y)$, with Ψ as in (11), i.e.

$$y = \Phi(\varrho_0(\xi), \eta).$$

Therefore

$$G(y, r, \varepsilon) = f(\Phi(r, \eta), \varepsilon) - \Phi(\xi, h(\xi, \varepsilon)),$$

Since $G_1(y, r) = \dfrac{\partial G}{\partial \varepsilon}(y, r, 0)$, we see that

$$G_1(y, r) = f_1(\Phi(r, \eta)) - \sum_{i=1}^{u} h_i(\xi)v_i^u(\xi).$$

Since $\varphi_0(r) = \Psi(\sigma_0(r), 0)$, we see that

$$G_1(\varphi_0(r), r) = f_1(\varphi_0(r)) - \sum_{i=1}^{u} h_i(\sigma_0(r))v_i^u(\sigma_0(r)).$$

$$\qquad\qquad\qquad\qquad\qquad\qquad\qquad\qquad\qquad\qquad\qquad\qquad\qquad\qquad\square$$

As in section 3, corollary 6, the fixed point $\overline{y}$ of $\mathcal{N}$ is of the form $\overline{y}(r, \varepsilon) = \varphi_0(r) + \varepsilon\overline{y}_1(r) + O(\varepsilon^2)$, with

$$\overline{y}_1(r) = -L(r)^{-1} \cdot G_1(\phi_0(r), r)$$

$$= \sum_{i,j=1}^{u} h_i(\sigma_0(r))(K_0(r))_{ij}^{-1}v_j(\sigma_0(r)) - K_0(r)^{-1}V^u(\sigma_0(r)) +$$

$$A_0(r)^{-1}V^c(\sigma_0(r)).$$

Therefore we have a good starting point for the Newton operator. Note that this version of the algorithm does not need to compute f_ε^{-1}, which in practical cases may turn out to be a very convenient feature.

5. The general case

There are several ways to extend algorithm GRAPH TRANSFORM to compute the invariant manifold $\mathbb{H}_\varepsilon$ of f_ε in the case where both normal expansion and normal contraction are present. One straightforward method is presented in section 5.1. To the best of our knowledge this is the first algorithm that computes invariant manifolds for which the normal dynamics exhibits both contraction and expansion.

A second algorithm first computes $\mathbb{W}^s(\mathbb{H}_\varepsilon)$ and $\mathbb{W}^u(\mathbb{H}_\varepsilon)$, the stable and unstable manifolds of $\mathbb{H}_\varepsilon$, see section 2.1, and determines $\mathbb{H}_\varepsilon$ as the intersection of these manifolds. We describe this version in section 5.2. A drawback is the need for a separate algorithm to compute the intersection of submanifolds.

5.1. Computing $\mathbb{H}_\varepsilon$

Combining the algorithms of section 3 and section 4 yields a hybrid method for the computation of $\mathbb{H}_\varepsilon$. As before $\mathbb{H}_\varepsilon$ is of the form

$$\mathbb{H}_\varepsilon = \{\Phi(r, \overline{h}_\varepsilon^s(r), \overline{h}_\varepsilon^u(r)) \mid r \in H_0\},$$

where $\overline{h}^s : H_0 \times \mathbb{R} \to \mathbb{R}^s$ and $\overline{h}^u : H_0 \times \mathbb{R} \to \mathbb{R}^u$ are C^1 functions. (Again we adopt the notation introduced in section 2.2.) The pair $(\overline{h}^s, \overline{h}^u)$ is the fixed point of the graph transform Γ_f, defined on the space of pairs (h_s, h_u) (as before endowed with a suitable norm that turns it into a complete metric space). The graph transform is of the form

$$\Gamma_f(h^s, h^u) = (\Gamma_f^s(h^s, h^u), \Gamma_f^u(h^s, h^u)).$$

The operator Γ_f^s, called the *forward graph transform*, is similar to the operator defined in section 3, whereas Γ_f^u, called the *backward graph transform*, is similar to the operator defined in section 4.

More precisely, for a section $h = (h^s, h^u) : H_0 \times \mathbb{R} \to \mathbb{R}^s \times \mathbb{R}^u$, there is a section $\eta = (\eta^s, \eta^u) : H_0 \times \mathbb{R} \to \mathbb{R}^s \times \mathbb{R}^u$, such that $f_\varepsilon(\text{graph}(h_\varepsilon)) = \text{graph}(\eta_\varepsilon)$. The forward graph transform is defined by

$$\Gamma_f^s(h) = \eta^s. \tag{29}$$

Similarly, there is a section $\xi = (\xi^s, \xi^u) : H_0 \times \mathbb{R} \to \mathbb{R}^s \times \mathbb{R}^u$, such that $f_\varepsilon^{-1}(\text{graph}(h_\varepsilon)) = \text{graph}(\xi_\varepsilon)$. The backward graph transform is then defined by

$$\Gamma_f^u(h) = \xi^u. \tag{30}$$

Again Γ_f is a contraction, whose fixed point defines the invariant manifold $\mathbb{H}_\varepsilon$.

The geometric conditions (29) and (30) are both equivalent to equations of the form $F(\tau, y^s, y^u, \varepsilon) = 0$, where $F : H_0 \times \mathbb{R}^s \times \mathbb{R}^u \times \mathbb{R} \to \mathbb{R}^d$ is a C^1 map, defined as in section 3, equation (4) and section 4, equation (19), respectively. Again Newton's method can be used to solve these equations. Although more involved, the details of the implementation are similar to those of the 'pure' versions of Newton's method. We omit these details, but refer to section 7.2 for an illustration of the performance of this approach.

5.2. Computing $\mathbb{W}^s(\mathbb{H}_\varepsilon)$ and $\mathbb{W}^u(\mathbb{H}_\varepsilon)$

We construct the stable manifold $\mathbb{W}^s(\mathbb{H}_\varepsilon)$ as the graph of a function $y_\varepsilon : H_0 \times \mathbb{R}^s \to \mathbb{R}^u$ (Actually, the domain of y_ε is a neighborhood of $H_0 \times \{0\}$ in $H_0 \times \mathbb{R}^s$). This graph is defined by

$$\mathrm{graph}(y_\varepsilon) = \{\Phi(r, x, y_\varepsilon(r, x)) \mid (r, x) \in H_0 \times \mathbb{R}^s\}.$$

The graph transform Γ_{f_ε} is defined by the following geometric condition:

$$f_\varepsilon^{-1}(\mathrm{graph}(y_\varepsilon)) = \mathrm{graph}(\Gamma_{f_\varepsilon}(y_\varepsilon)). \tag{31}$$

Apart from technical details, we are now in the context of section 3.1. Therefore, it is possible to translate condition (31) into an equation of the form (8). Solving this equation using algorithm NEWTON yields again a straighforward implementation of the graph transform, whose fixed point defines the invariant manifold $\mathbb{W}^s(\mathbb{H}_\varepsilon)$. Since the unstable manifold of $\mathbb{H}_\varepsilon$ is the stable manifold with respect to f_ε^{-1}, it can be computed similarly.

This approach yields an other method for the computation of $\mathbb{H}_\varepsilon$. Let us assume that the stable manifold $\mathbb{W}^s(\mathbb{H}_\varepsilon)$ has been computed as the graph of a map $\overline{y}_\varepsilon : H_0 \times \mathbb{R}^s \to \mathbb{R}^u$. The manifold $\mathbb{H}_\varepsilon \subset \mathbb{W}^s(\mathbb{H}_\varepsilon)$ can then be determined as the graph of a map $\overline{h}_\varepsilon : H_0 \to \mathbb{R}^s$, i.e. as a set of the form

$$\mathrm{graph}(\overline{h}_\varepsilon) = \{\Phi(r, \overline{h}_\varepsilon(r), \overline{y}_\varepsilon(r, \overline{h}_\varepsilon(r))) \mid r \in H_0\}.$$

In fact, restricting to the stable manifold $\mathbb{W}^s(\mathbb{H}_\varepsilon)$ brings us back to the special case of absence of normal expansion. The map $\overline{y}_\varepsilon$ establishes a diffeomorphism between $H_0 \times \mathbb{R}^s$ and $\mathbb{W}^s(\mathbb{H}_\varepsilon)$. Proceeding as in section 3, we introduce the graph transform Γ_{f_ε} on the space of families of maps (sections) $H_0 \to \mathbb{R}^s$. More precisely, for a section $h_\varepsilon : H_0 \to \mathbb{R}^s$ the section $\overline{h}_\varepsilon = \Gamma_{f_\varepsilon}(h_\varepsilon)$ is defined by the condition

$$\mathrm{graph}(\overline{h}_\varepsilon) = f_\varepsilon(\mathrm{graph}(h_\varepsilon)).$$

The section $\overline{h}_\varepsilon$ is well–defined, since $\mathrm{graph}(\overline{y}_\varepsilon)$ is f_ε–invariant. The Df_ε–invariant splitting of $T_{\mathbb{H}_\varepsilon}(\mathbb{R}^d)$ can be computed as in the case of absence of normal expansion.

5.3. Continuation: the computation of $\mathbb{N}^u(\mathbb{H}_\varepsilon) \oplus \mathbb{T}(\mathbb{H}_\varepsilon) \oplus \mathbb{N}^s(\mathbb{H}_\varepsilon)$

As explained in section 3.5, the algorithm can be applied in a continuation context, provided there is a subroutine that computes the Df_ε–invariant splitting $\mathbb{N}^u(\mathbb{H}_\varepsilon) \oplus \mathbb{T}(\mathbb{H}_\varepsilon) \oplus \mathbb{N}^s(\mathbb{H}_\varepsilon)$ of the tangent bundle $\mathbb{T}_{\mathbb{H}_\varepsilon}(\mathbb{R}^d)$. Such a subroutine can be obtained by applying some minor changes to the method of section 3.4.

To see this, consider the space $\Omega_s(\varepsilon_0)$, where an element $\omega \in \Omega_s(\varepsilon_0)$ maps a pair $(r, \varepsilon) \in H_0 \times [-\varepsilon_0, \varepsilon_0]$ continuously onto a linear map $\omega(r, \varepsilon) : \mathbb{N}_r^s(\mathbb{H}_0) \to$

$\mathbb{N}_r^u(\mathbb{H}_0) \oplus \mathbb{T}_r(\mathbb{H}_0)$. The stable normal bundle is obtained by iterating an operator $\mathcal{T}_s : \Omega_s(\varepsilon_0) \to \Omega_s(\varepsilon_0)$, defined by the requirement that, for $\overline{\omega} = \mathcal{T}_s(\omega)$,

$$\mathrm{graph}(\overline{\omega}_\varepsilon(r)) = Df_\varepsilon(\varphi_\varepsilon(r))^{-1}\mathrm{graph}(\omega_\varepsilon(\overline{\sigma}_\varepsilon(r))).$$

See also (16). As in section 3.4 one proves that $\mathcal{T}_s$ is a contraction, whose fixed point $\overline{\omega}_s$ defines $\mathbb{N}^s(\mathbb{H}_\varepsilon)$ by

$$\mathbb{N}_r^s(\mathbb{H}_\varepsilon) = \{\overline{\omega}_\varepsilon(r) \cdot u \oplus u \mid u \in \mathbb{N}_r^s(\mathbb{H}_0)\}.$$

The unstable bundle $\mathbb{N}^u(\mathbb{H}_\varepsilon)$ is obtained from the fixed point of a similarly defined contraction $\mathcal{T}_u$, defined on the space of linear maps

$$\omega(r,\varepsilon) : \mathbb{N}_r^u(\mathbb{H}_0) \to \mathbb{T}_r(\mathbb{H}_0) \oplus \mathbb{N}_r^s(\mathbb{H}_0),$$

that depend continuously on $(r,\varepsilon) \in H_0 \times \mathbb{R}$.

The tangent bundle $\mathbb{T}(\mathbb{H}_\varepsilon)$ is computed in two steps. First, we compute the space $\mathbb{N}_r^u(\mathbb{H}_\varepsilon) \oplus \mathbb{T}_r(\mathbb{H}_\varepsilon)$ from the fixed point of an operator $\mathcal{T}_{cu} : \Omega_{cu}(\varepsilon_0) \to \Omega_{cu}(\varepsilon_0)$, that is similar to the operator $\mathcal{T}_c$, introduced in section 3.4. Here $\Omega_{cu}(\varepsilon_0)$ consists of families of linear maps $\omega(r,\varepsilon) : \mathbb{N}_r^u(\mathbb{H}_\varepsilon) \oplus \mathbb{T}_r(\mathbb{H}_\varepsilon) \to \mathbb{N}_r^s(\mathbb{H}_\varepsilon)$, depending continuously on (r,ε). Then $\overline{\omega} = \mathcal{T}_{cu}(\omega)$ is defined by

$$\mathrm{graph}(\overline{\omega}_\varepsilon(r)) = Df_\varepsilon(\varphi_\varepsilon(\overline{\varrho}(r)))\mathrm{graph}(\omega_\varepsilon(\overline{\varrho}(r))).$$

The space $\mathbb{T}_r(\mathbb{H}_0) \oplus \mathbb{N}_r^s(\mathbb{H}_0)$ is computed similarly. Finally, the tangent space $\mathbb{T}_r(\mathbb{H}_\varepsilon)$ is determined by intersecting the spaces $\mathbb{N}_r^u(\mathbb{H}_\varepsilon) \oplus \mathbb{T}_r(\mathbb{H}_\varepsilon)$ and $\mathbb{T}_r(\mathbb{H}_0) \oplus \mathbb{N}_r^s(\mathbb{H}_0)$.

6. The discretized graph transform

6.1. The discretization problem

In implementations of the graph transform infinite dimensional objects need to be approximated by finite dimensional spaces, that have a finite representation. We sketch a feasible approximation scheme for manifolds and function spaces, thereby obtaining a discretized version of the graph transform. An important parameter of any approximation scheme is the *discretization error*. We derive a bound for the discretization error in terms of a geometric parameter of the approximation scheme. Numerical experiments corroborate this bound. First, however, we sketch the approximation scheme and state the main result concerning the discretization error. Related papers dealing with computational issues are e.g. [5, 6]. For a more complete survey, see [14].

$$
\begin{array}{ccc}
C^0(H_0,\mathbb{R}^s) & \xrightarrow{\ \ \Gamma\ \ } & C^0(H_0,\mathbb{R}^s) \\[2pt]
\Big\uparrow{\scriptstyle I} & & \Big\downarrow{\scriptstyle P} \\[2pt]
L(\mathbb{K},\mathbb{R}^s) & \xrightarrow{\ \ \overline{\Gamma}\ \ } & L(\mathbb{K},\mathbb{R}^s)
\end{array}
$$

Figure 3.
The discretized Graph Transform $\overline{\Gamma}$.

The manifold $\mathbb{H}_0$ is approximated by a finite simplicial complex $\mathcal{K}$, embedded in $\mathbb{R}^d$. E.g. if $\mathbb{H}_0$ is two-dimensional, such a complex is a polyhedral surface with affine triangles, whose vertices are points on $\mathbb{H}_0$. The discretization error is expressed in terms of the *mesh width* $m(\mathcal{K})$, viz the maximal diameter of any of the simplices of $\mathcal{K}$.

In our continuation scheme we increase the parameter ε by small steps. At this moment we fix the value of ε, suppressing ε from the notation (e.g. by writing Γ instead of Γ_{f_ε}, by considering sections as maps $H_0 \to \mathbb{R}^s$ instead of $H_0 \times [-\varepsilon_0, \varepsilon_0] \to \mathbb{R}^s$).

The domain of both the graph transform and the Newton operator are spaces of functions $H_0 \to \mathbb{R}^k$, with $k = s$ and $k = d$, respectively. These function spaces are approximated by the space $\mathcal{L}(\mathcal{K}, \mathbb{R}^k)$ of simplexwise linear functions. We shall describe how to construct this finite dimensional function space, together with a projection-like approximation map $\mathcal{P} : C^0(H_0, \mathbb{R}^k) \to \mathcal{L}(\mathbb{K}, \mathbb{R}^k)$, and an inclusion-like map $\mathcal{I} : \mathcal{L}(\mathbb{K}, \mathbb{R}^k) \to C^0(H_0, \mathbb{R}^k)$, a right inverse of $\mathcal{P}$. The *discretized graph transform* is the operator $\overline{\Gamma}$ on the space $\mathcal{L}(\mathcal{K}, \mathbb{R}^s)$, with $\overline{\Gamma} \approx \mathcal{P} \cdot \Gamma \cdot \mathcal{I}$. See also Figure 3. The definition of the graph transform implies that Γ can be extended as an operator on $C^0(H_0, \mathbb{R}^s)$. The implementation establishes a discretized graph transform $\overline{\Gamma}$, such that the diagram in Figure 3 commutes up to $O(m(\mathcal{K})^2)$; see section 6.4. More precisely, we construct an operator $\overline{\Gamma}$ on the space $\mathcal{L}(\mathbb{K}, \mathbb{R}^s)$ such that

$$
\|\overline{\Gamma}\mathcal{P}h - \mathcal{P}\Gamma h\|_{C^0} = O(m(\mathcal{K})^2). \tag{32}
$$

For (32) to hold we need to assume that f_0 and H_0 are C^3. In particular we assume that H_0 is a 3-normally hyperbolic invariant manifold of f_0. In particular we shall use that under these conditions the subspace $C_b^2(H_0, \mathbb{R}^s)$ of C^2-sections with bounded second derivatives is invariant under Γ.

The operator $\overline{\Gamma}$ is not guaranteed to be a contraction, so a priori it seems hard to speak of convergence of iteration under this operator. Fortunately, condition (32) turns out to be sufficient for obtaining a good estimate for the accuracy of this iteration process.

To see this, consider the *ideal sequence* h_n, defined by $h_n := \Gamma^n h_0$, with h_0 some well chosen initial value, cf section 3, remark 7. This sequence converges to the fixed point h_∞ of the graph transform, which defines the invariant manifold we set out to compute. The *computed sequence* $\overline{h}_n$ is defined by

$$\overline{h}_n = \begin{cases} \mathcal{P} h_0, & \text{if } n = 0, \\ \overline{\Gamma}\, \overline{h}_{n-1}, & \text{if } n > 0. \end{cases}$$

The next result gives information on when to stop iterating under $\overline{\Gamma}$.

Theorem 13 (Discretization Error). *Let f_0 be C^3, and let H_0 be a 3-normally hyperbolic invariant manifold of f_0. Let h_n and $\overline{h}_n$ be as above. Then*
Termination: *There is an $N \geq 0$ such that, for $n \geq N$:*

$$\|\overline{h}_{n+1} - \overline{h}_n\|_{C^0} = O(m(\mathcal{K})^2). \tag{33}$$

Approximation: *If (33) holds, then*

$$\|\mathcal{I}\overline{h}_n - h_\infty\|_{C^0} = O(m(\mathcal{K})^2). \tag{34}$$

As usual in numerical contexts, the constants implicit in (33) and (34) are not known in general. However, numerical experiments may give a clue on the size of the constants.

The termination clause of the theorem states that we may terminate the computation as soon as the distance between successive iterates under the implemented graph transform is of the order of the square of the mesh-width. The approximation clause guarantees that, upon termination, also the accuracy of the output is of the order of the square of the mesh-width.

In the remainder of this section we first describe the simplicial approximation scheme, subsequently prove theorem 13, and finally discuss the implementation of discretized versions of the Newton operator and the graph transform.

6.2. Simplicial approximation

First we describe how to approximate the invariant manifold $\mathbb{H}_0$. To this end we shall use a finite simplicial complex, whose vertices are points of $\mathbb{H}_0$. See e.g. [13] for a full account on simplicial complexes, and [8] for the use of simplicial complexes in approximation problems where non-structured grids are used.

Recall that a geometric c-simplex in $\mathbb{R}^d$, $0 \leq c \leq d$, is the convex hull of $c + 1$ points $p_0, p_1, \cdots, p_c$ in $\mathbb{R}^d$, that are in general position (i.e. they span a c-dimensional affine subspace of $\mathbb{R}^d$). This c-simplex is denoted by $\Delta(p_0, p_1, \cdots, p_c)$. The points p_i are called *vertices* of the simplex. The convex hull of any $j + 1$ of

the vertices is called a j-face of the simplex. Note that a c-simplex has exactly one c-face. Furthermore, the set of 0-faces coincides with the set of vertices.

By definition, every point $p \in \Delta(p_0, p_1, \cdots, p_c)$ can be written uniquely as $p = \sum_{i=0}^{c} \alpha_i(p)p_i$, with $\sum_{i=0}^{c} \alpha_i(p) = 1$. The scalars $\alpha_i(p)$, $i = 0, \cdots, c$, are called the *barycentric coordinates* of p (with respect to the simplex $\Delta(p_0, p_1, \cdots, p_c)$). Note that all barycentric coordinates of p are non-negative.

In this section we define a *(geometric) simplicial complex* in $\mathbb{R}^d$ as a finite collection $\mathcal{K}$ of geometric simplices in $\mathbb{R}^d$, satisfying the following conditions:

1. If Δ_j is a simplex of $\mathcal{K}$, and Δ_h is a h-face of Δ_j, then Δ_h is a simplex in $\mathcal{K}$;

2. If Δ and Δ' are simplices in $\mathcal{K}$, then their intersection $\Delta \cap \Delta'$ is either empty, or a common face of Δ and Δ'.

The union of all simplices is denoted by $\mathbb{K}$, and the set of all vertices is denoted by $\mathbb{K}_0$. We turn $\mathbb{K}$ into a metric space, using the metric induced from $\mathbb{R}^d$. The metric space $\mathbb{K}$ is called the underlying space of $\mathcal{K}$. The *mesh-width* of $\mathcal{K}$, denoted by $m(\mathcal{K})$, is the maximum of the diameters of its simplices.

We say that the simplicial complex $\mathcal{K}$ *supports* the invariant manifold $\mathbb{H}_0$ if all its vertices are points of $\mathbb{H}_0$ (i.e. $\mathbb{K}_0 \subset \mathbb{H}_0$), and the underlying space $\mathbb{K}$ is a topological manifold homeomorphic to $\mathbb{H}_0$. It is well known that every compact submanifold of $\mathbb{R}^d$ has a supporting simplicial complex, see e.g. [4]. In fact, the Hausdorff distance between $\mathbb{H}_0$ and the underlying space of a simplicial complex $\mathcal{K}$ supporting it can be made arbitrarily small by taking the mesh-width of $\mathcal{K}$ sufficiently small.

The latter property makes simplicial complexes attractive from the computational point of view, since they are finite, and yet approximate the invariant manifold arbitrarily well (with respect to the Hausdorff-metric).

Recall that the projection π_c maps a point p in a neighborhood of $\mathbb{H}_0$ onto the manifold H_0, by projecting $\Phi^{-1}(p) \in H_0 \times \mathbb{R}^s$ onto H_0. Assuming that the mesh-width of the supporting simplicial complex $\mathcal{K}$ is sufficiently small, the restriction of π_c to $\mathbb{K}$ is a homeomorphism, that is even smooth restricted to simplices of $\mathcal{K}$. With this assumption, the canonical map $\pi_c^* : C^0(H_0, \mathbb{R}^k) \to C^0(\mathbb{K}, \mathbb{R}^k)$, defined by $\pi_c^*(y) = y \cdot (\pi_c \mid \mathbb{K})$, is an isometry with respect to the sup-norms on its domain and range. The existence of this isometry enables us to identify continuous functions on H_0 with continuous functions on $\mathbb{K}$.

Let $\mathcal{L}(\mathbb{K}, \mathbb{R}^k)$ be the space of simplexwise linear functions, and let $I : \mathcal{L}(\mathbb{K}, \mathbb{R}^k) \to C^0(\mathbb{K}, \mathbb{R}^k)$ be the inclusion map. We shall use $k = s$ and $k = d$ in the algorithms. The latter map has a left-inverse P, defined as follows. Consider a point $p \in \mathbb{K}$, and let $\Delta(p_0, \ldots, p_c)$ be a simplex of $\mathcal{K}$ containing p. Then:

$$(Py)(p) = \sum_{i=0}^{c} \alpha_i(p)p_i. \tag{35}$$

Obviously P is a projection operator ($P^2 = P$). Furthermore, the approximation operator used in the implementation of the discretized graph transform is the

operator $\mathcal{P} : C^0(H_0, \mathbb{R}^k) \to \mathcal{L}(\mathbb{K}, \mathbb{R}^k)$, defined as the composite map $P \cdot \pi_c{}^*$. Since $\pi_c{}^*$ is an isometry, we see that the operator $\mathcal{P}$ has the following crucial property:

$$\|\mathcal{P}y_2 - \mathcal{P}y_1\|_{C^0} \le \|y_2 - y_1\|_{C^0}, \tag{36}$$

for all $y_1, y_2 \in C^0(H_0, \mathbb{R}^d)$.

The right inverse $\mathcal{I} : \mathcal{L}(\mathbb{K}, \mathbb{R}^k) \to C^0(H_0, \mathbb{R}^k)$ of $\mathcal{P}$ is the map $(\pi_c{}^{-1})^* \cdot I$. Again, using the fact that $\pi_c{}^*$ is an isometry, we see that

$$\|\mathcal{I}u_2 - \mathcal{I}u_1\|_{C^0} \le \|u_2 - u_1\|_{C^0}, \tag{37}$$

for all $u_1, u_2 \in \mathcal{L}(\mathbb{K}, \mathbb{R}^k)$.

The following result indicates that $\mathcal{I}$ is a left-inverse of $\mathcal{P}$ up to a quadratic term in the mesh-width, provided we restrict the domain of $\mathcal{P}$ to a suitable subset of $C^0(H_0, \mathbb{R}^k)$. Let $C_b^2(H_0, \mathbb{R}^k)$ be the space of C^2-maps whose second derivative is uniformly bounded (with respect to the Riemannian metric on H_0 and the Euclidean metric on $\mathbb{R}^k$).

Lemma 14. *For $y \in C_b^2(H_0, \mathbb{R}^k)$:*

$$\|y - \mathcal{I}\mathcal{P}y\|_{C^0} = O(m(\mathcal{K})^2). \tag{38}$$

Proof. Use the fact that $\pi_c{}^*$ is an isometry to restrict to C^2-functions defined on simplices of $\mathcal{K}$. The result then follows directly from [18], theorem 3.1.

The preceding result provides us with an upper bound on the discretization error we make when approximating a function by its $\mathcal{P}$-image. From condition (38) we derive:

Lemma 15. *For $u \in \mathcal{L}(\mathbb{K}, \mathbb{R}^k)$ and $y \in C_b^2(H_0, \mathbb{R}^k)$:*

$$\|y - \mathcal{I}u\|_{C^0} \le \|\mathcal{P}y - u\|_{C^0} + O(m(\mathcal{K})^2). \tag{39}$$

Proof. Apply (37) and (38), using
$$\|y - \mathcal{I}u\|_{C^0} \le \|y - \mathcal{I}\mathcal{P}y\|_{C^0} + \|\mathcal{I}\mathcal{P}y - \mathcal{I}u\|_{C^0}.$$

$\square$

6.3. Proof of Theorem 13

For the purpose of the proof we introduce constants $C_1, C_2 > 0$ such that, for $h \in C^0(\mathbb{K}, \mathbb{R}^s)$ and $\overline{h} \in \mathcal{L}(\mathbb{K}, \mathbb{R}^s)$:

$$\|\overline{\Gamma}\mathcal{P}h - \mathcal{P}\Gamma h\|_{C^0} \leq C_1 m(\mathcal{K})^2,$$
$$\|h - \mathcal{I}\overline{h}\|_{C^0} \leq \|\mathcal{P}h - \overline{h}\|_{C^0} + C_2 m(\mathcal{K})^2;$$

see (32) and (39).

Lemma 16. *Under the conditions of theorem 13 there is a constant $C > 0$ such that*

$$\|\overline{h}_n - \mathcal{P}h_n\|_{C^0} \leq Cm(\mathcal{K})^2. \tag{40}$$

Proof. We shall prove inductively that (40) holds, provided we take the constant C such that

$$C \geq \frac{C_1 + c_\Gamma C_2}{1 - c_\Gamma}. \tag{41}$$

Here c_Γ is the contraction factor of the graph transform.

First observe that (40) holds for $n = 0$, since $\overline{h}_0 = \mathcal{P}h_0$. Assume that (40) holds for n, then:

$$
\begin{aligned}
\|\overline{h}_{n+1} - \mathcal{P}h_{n+1}\|_{C^0} &= \|\overline{\Gamma h}_n - \mathcal{P}\Gamma h_n\|_{C^0} \\
&= \|\overline{\Gamma}\mathcal{P}\mathcal{I}\overline{h}_n - \mathcal{P}\Gamma h_n\|_{C^0} \\
&\leq \|\overline{\Gamma}\mathcal{P}\mathcal{I}\overline{h}_n - \mathcal{P}\Gamma\mathcal{I}\overline{h}_n\|_{C^0} + \|\mathcal{P}\Gamma\mathcal{I}\overline{h}_n - \mathcal{P}\Gamma h_n\|_{C^0} \\
&\leq C_1 m(\mathcal{K})^2 + c_\Gamma\|\mathcal{I}\overline{h}_n - h_n\|_{C^0} \\
&\leq C_1 m(\mathcal{K})^2 + c_\Gamma(C_2 m(\mathcal{K})^2 + \|\overline{h}_n - \mathcal{P}h_n\|_{C^0}) \\
&\leq (C_1 + c_\Gamma(C_2 + C))m(\mathcal{K})^2 \\
&\leq Cm(\mathcal{K})^2,
\end{aligned}
$$

provided $C_1 + c_\Gamma(C_2 + C) \leq C$. The latter condition is satisfied if we take C as indicated in (41). This completes the proof of the lemma. $\square$

Proof of Theorem 13.

Termination: This is an immediate consequence of lemma 16, using

$$\|\overline{h}_{m+1} - \overline{h}_m\|_{C^0} \leq \|\overline{h}_{m+1} - \mathcal{P}h_{m+1}\|_{C^0} + \|\overline{h}_m - \mathcal{P}h_m\|_{C^0} + \|h_{m+1} - h_m\|_{C^0}.$$

Note that $\|h_{m+1} - h_m\|_{C^0}$ is arbitrarily small for n sufficiently large.

Approximation:

$$\|I\overline{h}_m - h_\infty\|_{C^0} \leq \|\mathcal{I}\overline{h}_m - h_m\|_{C^0} + \|h_m - h_\infty\|_{C^0}$$
$$\leq C_2 m(\mathcal{K})^2 + \|\mathcal{P}u_m - \overline{h}_m\|_{C^0} + \|h_m - h_\infty\|_{C^0}$$
$$\leq (C_2 + C)m(\mathcal{K})^2 + \|h_m - h_\infty\|_{C^0}.$$

Here C is as in lemma 16. Furthermore:

$$\|h_m - h_\infty\|_{C^0} \leq \sum_{i=m}^{\infty} \|h_i - h_{i+1}\|_{C^0}$$
$$\leq \sum_{i=m}^{\infty} c_\Gamma^i \|h_m - h_{m+1}\|_{C^0}$$
$$\leq \frac{1}{1 - c_\Gamma} \|h_m - h_{m+1}\|_{C^0}.$$

Finally:

$$\|h_m - h_{m+1}\|_{C^0} \leq \|h_{m+1} - \mathcal{I}\overline{h}_{m+1}\|_{C^0} + \|\mathcal{I}\overline{h}_{m+1} - \mathcal{I}\overline{h}_m\|_{C^0} + \|\mathcal{I}\overline{h}_m - h_{m+1}\|_{C^0}$$
$$\leq C_2 m(\mathcal{K})^2 + \|\mathcal{P}h_{m+1} - \overline{h}_{m+1}\|_{C^0} + \|\overline{h}_{m+1} - \overline{h}_m\|_{C^0}$$
$$+ C_2 m(\mathcal{K})^2 + \|\mathcal{P}h_m - \overline{h}_m\|_{C^0}$$
$$\leq 2(C_2 + C)m(\mathcal{K})^2 + \|\overline{h}_{m+1} - \overline{h}_m\|_{C^0}$$
$$\leq (2C_2 + 3C)m(\mathcal{K})^2.$$

Combining the above estimates we get
$$\|\mathcal{I}\overline{h}_m - h_\infty\|_{C^0} \leq \left(C_2 + C + \frac{2C_2 + 3C}{1 - c_\Gamma}\right) m(\mathcal{K})^2.$$

$$\square$$

6.4. Implementation of the discretized graph transform

To complete the discussion on the discretization problem we only have to describe the construction of the discretized version $\overline{\Gamma}$ of the graph transform, satisfying (32).

As the pseudo-code of the algorithm GRAPH TRANSFORM of section 3 reveals, application of the graph transform boils down to iterating the Newton operator. Observe that theorem 13 gives the termination condition for the iterative application of $\overline{\Gamma}$. A similar result settles the termination condition for iteration under the Newton operator in algorithm GRAPH TRANSFORM. So we focus on the construction of the discretized version $\overline{\mathcal{N}}$ of the Newton operator, satisfying

$$\|\overline{\mathcal{N}}\mathcal{P}y - \mathcal{P}\mathcal{N}y\|_{C^0} = O(m(\mathcal{K})^2), \tag{42}$$

for C^2-functions $y : \mathbb{K} \to \mathbb{R}^d$ with bounded second derivatives, cf. the conditions of theorem 13.

We now indicate how to construct a discretized version of the map $\Phi : H_0 \times \mathbb{R}^s \to \mathbb{R}^d$, that identifies a neighborhood of $H_0 \times \{0\}$ with a neighborhood of $\mathbb{H}_0$ in $\mathbb{R}^d$; see section 2. To this end we first introduce discretized versions of the affine spaces $\mathbb{N}_x^s(\mathbb{H}_0)$ of $\mathbb{R}^d$. More specifically, consider $x \in \mathbb{K}$, and assume x belongs to the simplex $\Delta(p_0, \dots, p_c)$. Then $\overline{\mathbb{N}}_x^s(\mathbb{K})$ is the space spanned by the basis $\overline{u}_1(x), \dots, \overline{u}_s(x)$, defined by

$$\overline{u}_i(x) = \sum_{j=0}^c \alpha_j(x) u_i(\pi_c(p_j)),$$

for $i = 1, \dots, s$. Observe that $\overline{u}_i(x) = u_i(\pi_c(x))$ in case x is a vertex of $\mathbb{K}$. Then $\overline{\Phi} : \mathbb{K} \times \mathbb{R}^s \to \mathbb{R}^d$ is defined by

$$\overline{\Phi}(x, \eta) = \sum_{i=1}^s \eta_i \overline{u}_i(x).$$

Note that $\overline{u}_i = \mathcal{P} u_i$. In view of the conditions stated in theorem 13, the functions u_i are C^2, and have bounded second derivatives (since H_0 is compact). Therefore, lemma 14 allows us to conclude

$$\|\overline{\Phi}(x, \eta) - \Phi(\pi_c(x), \eta)\| = O(m(\mathcal{K})^2). \tag{43}$$

From this we easily construct the discretized versions $\overline{\pi}_c$ and $\overline{\pi}_s$ of the projections π_c and π_s. More precisely, for $y \in \mathbb{R}^d$:

$$y = \overline{\Phi}(x, \eta) \text{ iff } x = \overline{\pi}_c(y) \text{ and } \eta = \overline{\pi}_s(y).$$

The constructions of the discretized versions of the remaining objects in algorithm DISCRETIZED NEWTON below are straightforward. Condition (43) guarantees that the discretized Newton operator $\overline{\mathcal{N}}$ satisfies (42). For completeness we give the complete pseudo-code for the implementation of $\overline{\mathcal{N}}$.

Algorithm DISCRETIZED NEWTON
Input: $\overline{y} \in \mathcal{L}(\mathbb{K}, \mathbb{R}^d)$, $\overline{y} = y$ for y near y_0 as above.
Output: $\overline{\mathcal{N}}\overline{y} \in \mathcal{L}(\mathbb{K}, \mathbb{R}^d)$ satisfying (42).
forall $r \in \mathbb{K}_0$ **do**
1               $x \leftarrow \overline{\pi}_c(\overline{y}(r))$
                Comment: $x \in \mathbb{K}$ and $\overline{y}(r) - x \in \overline{\mathbb{N}}_x^s(\mathbb{K})$
2               $\eta \leftarrow \overline{\iota}_x(\overline{y}(r) - x)$
                Comment: $\overline{y}(r) = \overline{\Phi}(x, \eta)$
3               $Y \leftarrow \overline{F}(\overline{\varrho}_o(x), \eta, r)$
                Comment: $Y = \overline{G}(\overline{y}(r), r)$
4               $Y^c \leftarrow \overline{\Pi}_r^c(Y)$
                $Y^s \leftarrow \overline{\Pi}_r^s(Y)$
5               $\overline{\mathcal{N}}\overline{y}(r) \leftarrow \overline{y}(r) - Y^c + Y^s$

Remark 17. The use of the space of simplexwise linear functions $\mathcal{L}(\mathbb{K}, \mathbb{R}^k)$ allows us to compute with accuracy $O(m(\mathcal{K})^2$. Higher accuracy can be obtained by using non-linear splines, provided we assume sufficient regularity and normal hyperbolicity. The feasibility of such approximations is subject of future research.

7. Numerical examples

Finally we show the performance of our algorithm in some applications, all of which fall in the continuation context described in section 3.5. For continuation techniques in a different context: See e.g. [9, 7].

It turns out that in all examples the invariant manifolds are normally hyperbolic with respect to the Riemannian metric that coincides with the standard euclidean metric of the ambient space. Obviously, one cannot assume this to be true in general. More examples are contained in [2, 14].

7.1. The fattened Thom map

First we illustrate the algorithm in the simple case of absence of normal expansion, cf section 3. To this end consider the diffeomorphism f_ε, defined on $(\mathbb{R}/2\pi\mathbb{Z})^2 \times \mathbb{R}$ by $f_\varepsilon(x, y, z) = (2x + y + \varepsilon z, x + y + \varepsilon z, az + \varepsilon \sin x)$. (We may consider f_ε as a diffeomorphism defined on $\mathbb{R}^3$ that is periodic in the first two coordinates.)

We fix the constant $a > 0$, such that the system f_0 has a normally hyperbolic invariant torus $\mathbb{H}_0 := (\mathbb{R}/2\pi\mathbb{Z})^2 \times \{0\}$ (more specifically, we take $a = 0.1$; normal hyperbolictiy can be checked by computing of the eigenvalues of Df_ε at $(0, 0, 0) \in \mathbb{H}_\varepsilon$.) This invariant torus may be considered as the image of $H_0 = (\mathbb{R}/2\pi\mathbb{Z})^2$ under the canonical embedding $\varphi_0(x, y) = (x, y, 0)$. Note that the restriction of f_0 to this torus is the Thom automorphism $(x, y) \mapsto (2x + y, x + y)$. The tangent plane of $\mathbb{H}_0$ at $(x, y, 0)$ is defined by $z = 0$, the space $\mathbb{N}^s_{(x,y,0)}(\mathbb{H}_0)$ is spanned by the unit vector in the z–direction.

In figure 4 (left: top and bottom) the initial data, viz $\mathbb{H}_0$ and the splitting $\mathbb{T}(\mathbb{H}_0) \oplus \mathbb{N}^s(\mathbb{H}_0)$, is shown. The normally hyperbolic torus $\mathbb{H}_0$ is represented by a square mesh of 50×50 equidistant points.

Numerically we detect that for $\varepsilon \approx 0.4699$ the normal behavior of f_ε ceases to dominate the tangential behavior, viz $\mu_s \approx 1$, cf section 2.1.

Consequently, we can expect that the continuation cannot go past $\varepsilon = 0.4699$. Our algorithm computes a family $\mathbb{H}_\varepsilon$ of invariant tori, for ε ranging from 0 to 0.4698, with an estimated accuracy of order 10^{-4}. The initial increment of the continuation parameter ε is set to 0.02, but is adjusted (viz made smaller) as the normal hyperbolicity gets weaker. The square mesh, representing $\mathbb{H}_\varepsilon$, is fixed during the computations. Figure 4 (right: top and bottom) shows the last invariant torus we were able to compute. For this value of ε the contraction factor of one of
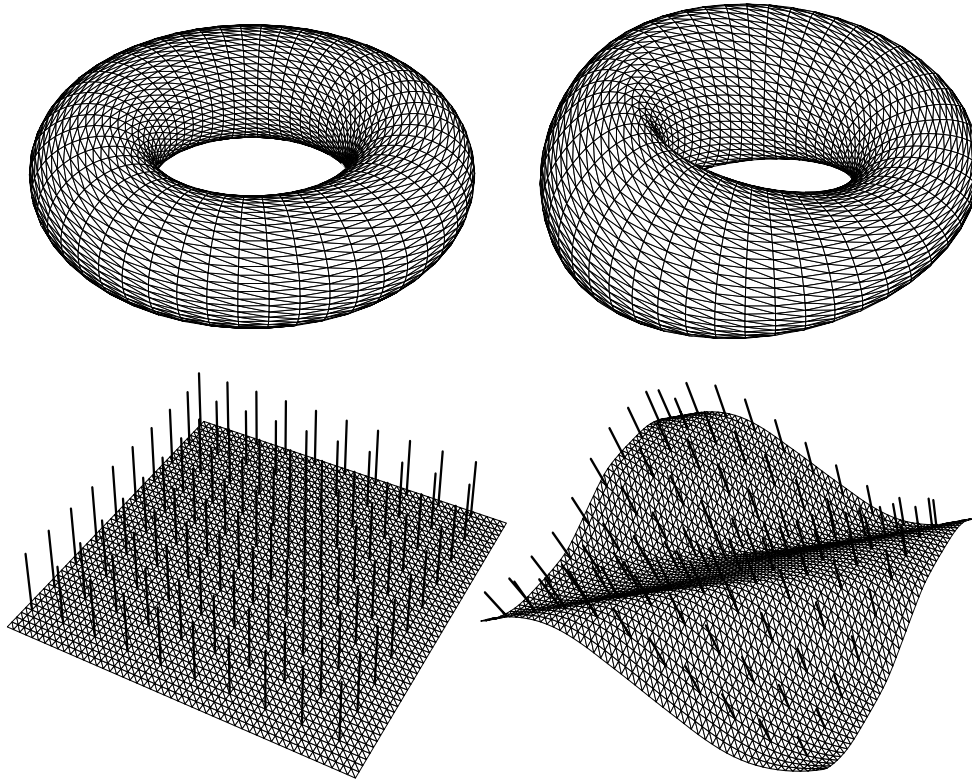
Figure 4.
The continuation of the Thom map in $\mathbb{R}^3$: $a = 0.1$; ε runs from 0 to 0.4698.
Top: The torus for $\varepsilon = 0$ (left) and $\varepsilon = 0.4698$ (right) embedded in $\mathbb{R}^3$.
Bottom: The data with the normal directions drawn at some of the mesh points for $\varepsilon = 0$ (left)
and $\varepsilon = 0.4698$ (right).

the operators Γ_{f_ε}, see section 3.1, $\mathcal{T}_c$, or $\mathcal{T}_s$; see section 3.4, is close to 1. In other
words, the torus $\mathbb{H}_\varepsilon$ is about to lose its 1–normal hyperbolicity.

Numerical Analysis

The performance of the algorithm is controled by the value of certain constants;
see table 1 for a list of constants in the current example. The algorithm estimates
the contraction factor of the operators involved in the computation of the invariant
manifold $\mathbb{H}_\varepsilon$ and the invariant splitting $\mathbb{N}^s(\mathbb{H}_\varepsilon) \oplus \mathbb{T}(\mathbb{H}_\varepsilon)$ of its tangent bundle. We
allow the process to settle down in 6 iteration steps before we start measuring the

contraction factor. With a maximal value of 0.98 for this estimated contraction factor, we can reach $\varepsilon = 0.4698$ for which, however, it takes already 515 iterations to compute the normal direction $\mathbb{N}^s(\mathbb{H}_\varepsilon)$.

Table 1.

Constants controling the performance of the algorithm (Thom map).

Accuracy:	10^{-4}
Accuracy Newton:	10^{-6}
Maximal contraction factor:	0.98
Initial continuation step:	0.02
Minimal continuation step:	10^{-4}
Minimal number of iterations:	6

The numerical performance of the continuation process is shown in Table 2. We indicate the number of steps needed for the Newton method, and the estimated contraction factors of the graph transform Γ_{f_ε}, computing $\mathbb{H}_\varepsilon$, and the invariant splitting. The contraction factor of the operator $\mathcal{T}_c$, computing the tangent direction $\mathbb{T}(\mathbb{H}_\varepsilon)$, turns out to be equal to the contraction factor of $\mathcal{T}_s$, that computes the normal direction $\mathbb{N}^s(\mathbb{H}_\varepsilon)$.

Table 2.

The continuation process for $a = 0.1$; the continuation parameter ε runs from 0 to 0.4698. The table shows the relation between ε, the number of iterations N in the Newton method and the contraction factors for the computation of the torus $\mathbb{H}_\varepsilon$ and its invariant splitting $\mathbb{T}(\mathbb{H}_\varepsilon) + \mathbb{N}^s(\mathbb{H}_\varepsilon)$.

ε	N	Γ_{f_ε}	$\mathcal{T}_c/\mathcal{T}_s$	ε	N	Γ_{f_ε}	$\mathcal{T}_c/\mathcal{T}_s$
0.02	3	0.100	0.26	0.4675	16	0.071	0.87
0.06	3	0.099	0.27	0.4688	16	0.069	0.91
0.14	4	0.094	0.28	0.4694	16	0.069	0.94
0.3	6	0.089	0.36	0.4697	16	0.068	0.96
0.46	15	0.084	0.76	0.4698	16	0.068	0.98
0.465	16	0.079	0.82				

The convergence itself is visualized in figure 5. Near the fixed point, the contraction behaves like its linear part at the fixed point. Therefore we expect each of our plots to approach a horizontal line, whose vertical coordinate is the contraction factor. This is corroborated by the numerical results depicted in figure 5.

7.2. The fattened Arnol′d family

We now apply the general version of the algorithm, sketched in section 5. Consider the *fattened Arnol′d family* of diffeomorphisms on $(\mathbb{R}/2\pi\mathbb{Z}) \times \mathbb{R}^2$:

$$f_\varepsilon \begin{pmatrix} x \\ y \\ z \end{pmatrix} = \begin{pmatrix} x + a + \varepsilon(y + z/2 + \sin x) \\ b(y + \sin x) \\ c(y + z + \sin x) \end{pmatrix}, \qquad (44)$$
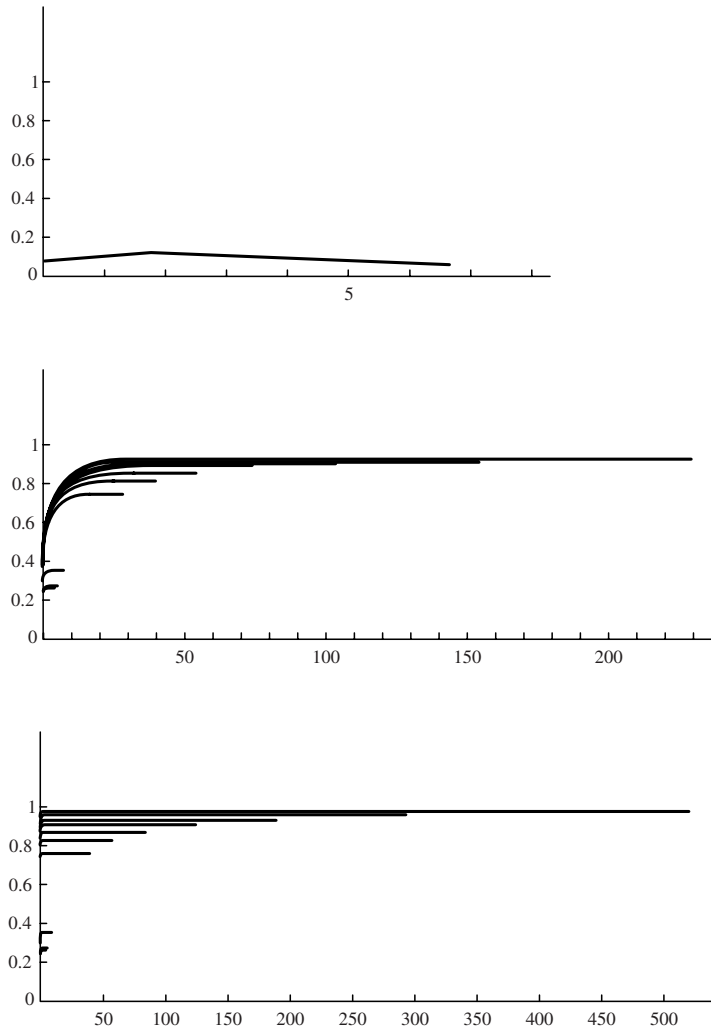
Figure 5.
The convergence process of the Thom map in $\mathbb{R}^3$: $a = 0.1$; ε is increasing from bottom to top. The pictures show the number of iterations versus the estimated contraction factor.
Top down the convergence processes for the computations of $\mathbb{H}_\varepsilon$, $\mathbb{T}(\mathbb{H}_\varepsilon)$ and $\mathbb{N}^s(\mathbb{H}_\varepsilon)$ are shown respectively.

where $x \in \mathbb{R}/2\pi\mathbb{Z}$. See also Broer, Simó and Tatjer [3] for a similar diffeomorphism on $\mathbb{S}^1 \times \mathbb{R}$. The constant a is defined modulo 2π, and the system f_0 has an invariant circle $\mathbb{H}_0$, on which the dynamics is (conjugate to) the rigid rotation $\sigma_0(x) = x + a$. Furthermore, for $0 < b < 1$ and $c > 1$, the invariant circle $\mathbb{H}_0$ is 1–normally hyperbolic with one–dimensional stable and unstable directions. (In
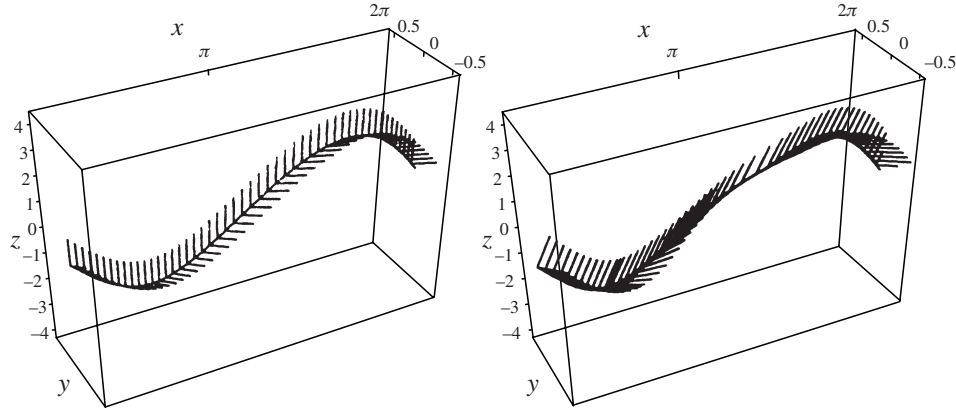
Figure 6.
The invariant circle of the fattened Arnol'd family; $a = 0.1$, $b = 0.3$ and $c = 2.4$. Left the initial data for $\varepsilon = 0$ and right the circle for $\varepsilon = 0.7125$. The normal directions are drawn for 50 mesh points (left) and 51 mesh points (right).

our example we take $a = 0.1$, $b = 0.3$ and $c = 2.4$.) Consequently, the system has a 1–normally hyperbolic invariant circle $\mathbb{H}_\varepsilon$, for small ε. The dynamics of $f_\varepsilon \mid \mathbb{H}_\varepsilon$ is either periodic or quasi–periodic, the periodic behavior being characterized by the existence of so–called Arnol'd tongues, cf [1].

It is easy to represent the embedding φ_0 by determining an explicit parametrization of the invariant circle $\mathbb{H}_0$. Furthermore, the Df_0–invariant splitting $\mathbb{N}^s(\mathbb{H}_0) \oplus \mathbb{T}(\mathbb{H}_0) \oplus \mathbb{N}^u(\mathbb{H}_0)$ can also be determined explicitly; see figure 6 (left). The invariant circle $\mathbb{H}_0$ is represented by a mesh of 50 points.

Two saddles appear on the invariant circle in a saddle–node bifurcation for $\varepsilon = 0.49$. Computation of the eigenvalues at these saddles reveals that for $\varepsilon \approx 0.7761$ the normal behavior of f_ε ceases to dominate the tangential behavior. So ε cannot increase beyond 0.7761 during the continuation process. In fact, the algorithm computes a family $\mathbb{H}_\varepsilon$ of invariant circles, for ε ranging from 0 to 0.7125, with an estimated accuracy of order 10^{-4}. The initial increment of the continuation parameter ε is set to 0.2, and is adjusted (viz made smaller) as the normal hyperbolicity gets weaker. A picture of the invariant circle for $\varepsilon = 0.7125$ is shown in figure 6 (right). Notice the change in the normal directions near the inflection point, compared to the initial circle (left).

Numerical Analysis

For this numerical experiment we implemented the algorithm presented in section 5.1. The initial continuation step size was set to 0.2, the other constants controling the numerical performance were taken as in table 1.

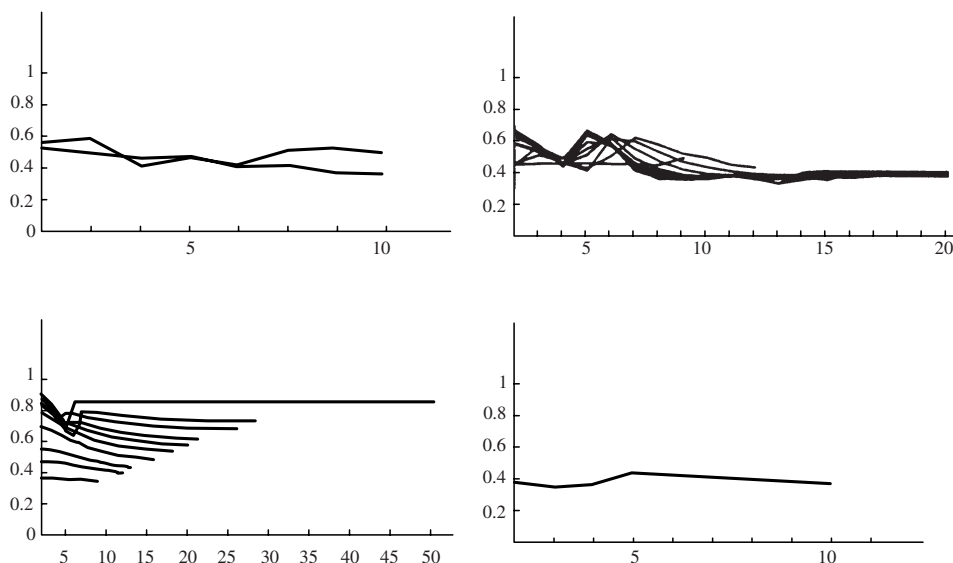Recall from section 5.1 that the graph transform Γ_{f_ε} is composed of the forward

Figure 7.
The convergence process of the Arnol′d map: $a = 0.1$, $b = 0.3$ and $c = 2.4$. The pictures show the number of iterations versus the estimated contraction factor.
Top left shows two typical steps in the computation of $\mathbb{H}_\varepsilon$. Top right, bottom left and bottom right show the continuation processes for $\mathbb{T}(\mathbb{H}_\varepsilon)$, $\mathbb{N}^s(\mathbb{H}_\varepsilon)$ and $\mathbb{N}^u(\mathbb{H}_\varepsilon)$, respectively.

graph transform $\Gamma^s_{f_\varepsilon}$ and the backward graph transform $\Gamma^u_{f_\varepsilon}$. Table 3 summarizes the numerical behavior of these operators. Here N_s and N_u are the number of iterations of the Newton operator associated with these operators. (The mesh did not change significantly; only one point was added for the last two continuation steps.)

Part of the iteration process is visualized in Figure 7 (top left).

We note in passing that, in case the inverse map f_ε^{-1} is known explicitly, the backward graph transform $\Gamma^u_{f_\varepsilon}$ can be replaced with the forward graph transform $\Gamma^s_{f_\varepsilon^{-1}}$. We repeated the experiment with this version of the algorithm, and observed that the Newton method in both the forward and the backward graph transform needs only 5 to 7 steps. Probably for this reason, the continuation could go as far as $\varepsilon = 0.7406$.
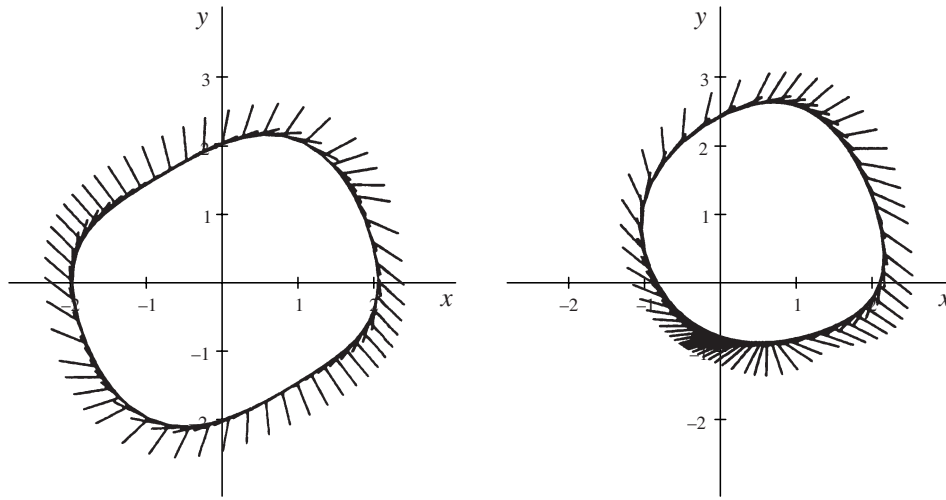
Figure 8.
The invariant circle of the forced Van der Pol oscillator: $a = 0.4$, $\omega = 0.9$; ε runs from 0 to 0.3609. The initial circle (left) and the last circle (right).

The forced Van der Pol oscillator

Finally, we show how to apply the algorithm to compute the invariant manifold of the Poincaré first–return map of a continuous system.

To this end consider the forced Van der Pol oscillator X_ε, a continuous system on the generalized phase space $\mathbb{R}^2 \times \mathbb{R}/2\pi\mathbb{Z}$:

$$
\begin{cases}
\dot{x} = y \\
\dot{y} = -x - a(x^2 - 1)y + \varepsilon \cos t \\
\dot{t} = \omega.
\end{cases}
\tag{45}
$$

Here a and ω are constants, with $a > 0$ and $0 < \omega < 2\pi$, and ε is the continuation parameter. We naturally get a diffeomorphism on the x, y–plane by considering the Poincaré map P_ε, the stroboscopic map of the 2π–periodic forcing term $\varepsilon \cos t$. For $\varepsilon = 0$ there is no forcing, so the the system decouples to the autonomous two–dimensional system, called the free Van der Pol oscillator:

$$
\begin{cases}
\dot{x} = y \\
\dot{y} = -x - a(x^2 - 1)y.
\end{cases}
\tag{46}
$$

This planar autonomous system has a closed orbit, which is attracting for $a < 2$, see [11]. (In this example we take $a = 0.4$ and $\omega = 0.9$.) The closed orbit corresponds to an invariant circle of P_0, that is normally hyperbolic.
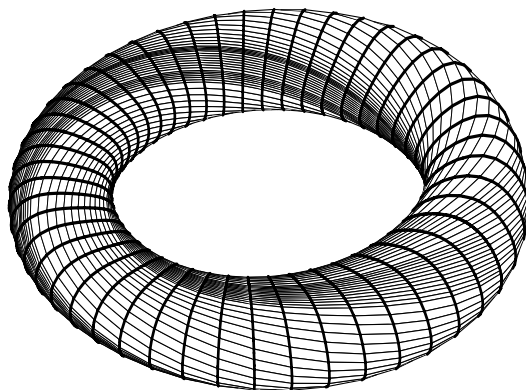
Figure 9.
The invariant torus of the forced Van der Pol oscillator; $a = 0.4$, $\omega = 0.9$ and $\varepsilon = 0.3609$. We
identified $t = 0$ with $t = 2\pi$ and embedded the torus in $\mathbb{R}^3$.

Considered in the phase space $\mathbb{R}^2 \times \mathbb{R}/2\pi\mathbb{Z}$ of (45), this closed orbit yields an
attracting invariant 2–torus. Due to normal hyperbolicity, the circle and, hence,
the torus, is persistent for small values of ε.

The invariant circle $\mathbb{H}_0$ of P_0 is a globally attracting limit cycle, and can there-
fore be computed by forward iteration of the planar system (46). A mesh of 50
points represents $\mathbb{H}_0$. The invariant splitting $\mathbb{T}_{\mathbb{H}_0}(\mathbb{R}^2) = \mathbb{T}(\mathbb{H}_0) \oplus \mathbb{N}^s(\mathbb{H}_0)$ is found
by computing the eigenvectors of $D\phi_T(r)$, for $r \in \mathbb{H}_0$, where ϕ_T is the time T–map
of the autonomous system (46), and T is the period of the limit cycle. The initial
data is shown in figure 8 (left).

Numerical computations show that for $\varepsilon \approx 0.3634$ a saddle on the circle and a
source inside it dissapear due to a *normal* saddle–node bifurcation, destroying the
normally hyperbolic invariant circle. (The saddle is born earlier in the continuation
process, due to a saddle–node bifurcation on the circle.) Hence, we expect the
continuation process to break down for $\varepsilon \approx 0.3634$.

The algorithm computes the family $\mathbb{H}_\varepsilon$ of invariant circles for ε ranging from
0 to 0.3609, with an estimated accuracy of 10^{-4}. Figure 8 (right) shows the last
invariant circle we were able to compute. The algorithm refines the mesh and
decreases the step size of the continuation parameter as the normal hyperbolicity
gets weaker. Due to the automatic refinement of the mesh the final circle consists
of 61 points. Figure 9 shows the result of saturating the final invariant circle,
by computing the X_ε–orbit of every mesh point. Representing each orbit by 50
points, corresponding to fixed length time intervals, we obtain 50 circles as an ap-
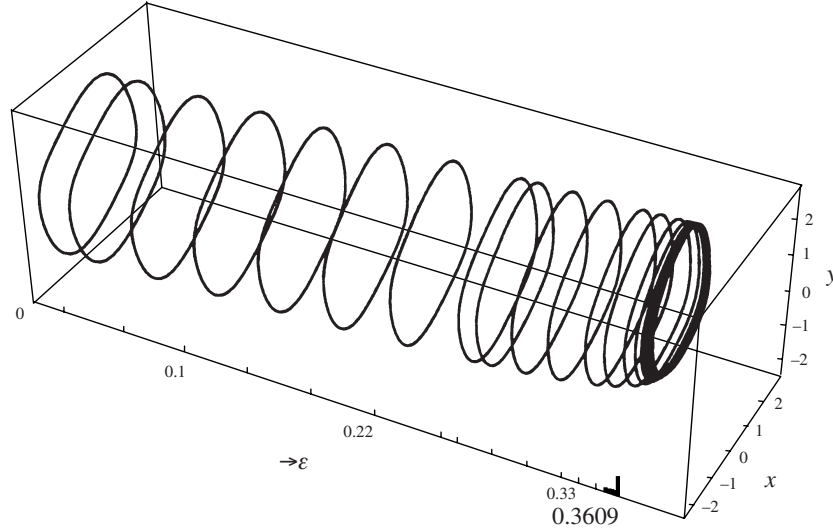proximation of the X_ε–invariant torus in the generalized phase space $\mathbb{R}^2 \times \mathbb{R}/2\pi\mathbb{Z}$.

Figure 10.
A branch of invariant circles for the Poincaré map of the forced Van der Pol oscillator: $a = 0.4$ and $\omega = 0.9$; ε ranges from 0 to 0.3609. The circles are drawn as a function of ε.

Table 3.
The continuation process for $a = 0.1$, $b = 0.3$ and $c = 2.4$; the continuation parameter ε runs from 0 to 0.7125.
The table shows the relation between ε and the numerical behavior of the forward and backward graph transforms involved in the computation of $\mathbb{H}_\varepsilon$. N_s and N_u are the numbers of iterations needed for Newton's method.

ε	N_s	$\Gamma^s_{f_\varepsilon}$	N_u	$\Gamma^u_{f_\varepsilon}$	ε	N_s	$\Gamma^s_{f_\varepsilon}$	N_u	$\Gamma^u_{f_\varepsilon}$
0.2	5	0.41	9	0.44	0.675	5	0.31	9	0.42
0.4	5	0.41	7	0.44	0.6875	5	0.31	10	0.43
0.5	5	0.36	7	0.41	0.7	5	0.31	12	0.48
0.6	5	0.36	8	0.39	0.7063	5	0.34	19	0.50
0.65	5	0.33	9	0.39	0.7125	5	0.35	36	0.53

Numerical Analysis

The constants controling the performance of the algorithm are taken as in table 7.1. In Figure 10 the continuation steps are shown.

Figure 11 reflects the performance of the algorithm for certain values of the continuation parameter. Again we separately depict the numerical results for each of the operators Γ_{f_ε}, $\mathcal{T}_c$ and $\mathcal{T}_s$. The Newton method that is integrated in the
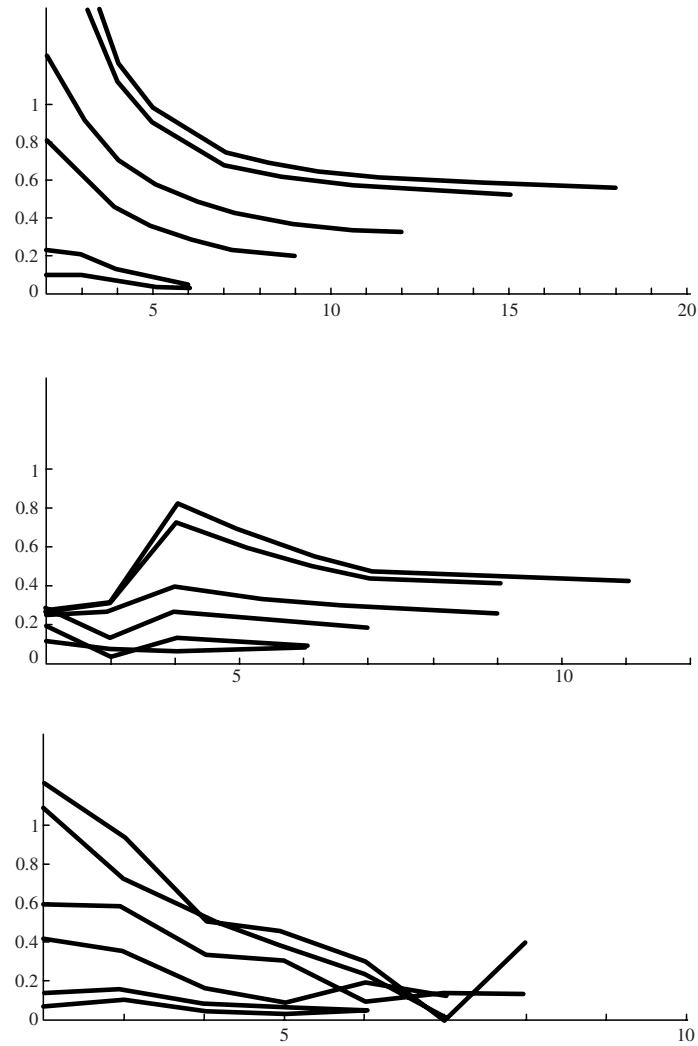
Figure 11.
Part of the convergence process of the Van der Pol oscillator: $a = 0.4$ and $\omega = 0.9$; $\varepsilon = 0.1$, 0.22, 0.33, 0.35, 0.36 and 0.3609 from bottom to top. The pictures show the number of iterations versus the estimated contraction factor.
Top down the convergence processes for the computation of $\mathbb{H}_\varepsilon$, $\mathbb{T}(\mathbb{H}_\varepsilon)$ and $\mathbb{N}^s(\mathbb{H}_\varepsilon)$ are shown respectively.

iteration of the graph transform Γ_{f_ε}, uses 4 to 8 steps to converge, depending on the size of the continuation step and the size of the continuation parameter ε.

References

[1] V. I. Arnol'd, Small denominators I, *Transl. Amer. Math. Soc., 2nd series* **46** (1965), 213–284.

[2] H. W. Broer, H. M. Osinga and G. Vegter, On the computation of normally hyperbolic invariant manifolds, In: H. W. Broer, S. A. van Gils, I. Hoveijn, and F. Takens, editors *Progress in Nonlinear Differential Equations and Their Applications*, vol. 19, pp. 423–447. Birkhäuser Verlag, Basel/Switzerland, 1996.

[3] H. W. Broer, C. Simó, and J. C. Tatjer, Towards global models near homoclinic tangencies of dissipative diffeomorphisms, Preprint University of Barcelona.

[4] S. S. Cairns, A simple triangulation method for smooth manifolds, *Bull. Amer. Math. Soc.* **67** (1961), 389–390.

[5] L. Dieci and J. Lorenz, Computation of invariant tori by the method of characteristics, *SIAM J. Numer. Anal.* **32** (5) (1995), 1436–1474.

[6] L. Dieci, J. Lorenz, and R. D. Russel, Numerical calculation of invariant tori, *SIAM J. Sci. Stat. Comput.*, **12** (3) (1991), 607–647.

[7] E. J. Doedel and J. P. Kernévez, AUTO:Software for continuation and bifurcation problems in ordinary differential equations, Technical report, California Institute of Technology, Pasadena, 1986. Applied Mathematics Report.

[8] H. Edelsbrunner, Modeling with simplicial complexes: Topology, geometry, and algorithms. In: *Proc. 6th Canad. Conf. Comput. Geom.* 1994, pp. 36–44.

[9] M. J. Friedman and E. J. Doedel, Numerical computation and continuation of invariant manifolds connecting fixed points, *SIAM J. Numer. Anal.* **28** (3) (1991), 789–808.

[10] M. W. Hirsch, C. Pugh, and M. Shub, *Invariant Manifolds*, vol. 583 of *Lecture Notes in Mathematics*, Springer-Verlag, 1977.

[11] M. W. Hirsch and S. Smale, *Differential Equations, Dynamical Systems, and Linear Algebra*, Academic Press, New York, 1974.

[12] A. J. Homburg, H. M. Osinga, and G. Vegter, On the computation of invariant manifolds of fixed points, *Z. Angew. Math. Phys.* **46** (1995), 171–187.

[13] S. R. F. Maunder, *Algebraic Topology*, Van Nostrand Reinhold, London, 1970.

[14] H. M. Osinga, *Computing Invariant Manifolds — Variations on the Graph Transform*, PhD thesis, University of Groningen, 1996.

[15] J. Palis and F. Takens, *Hyperbolicity & Sensitive Chaotic Dynamics at Homoclinic Bifurcations*, vol. 35 of *Cambridge Studies in Advanced Mathematics*, Cambridge University Press, 1993.

[16] D. Ruelle, *Elements of Differentiable Dynamics and Bifurcation Theory*, Academic Press, New York, 1989.

[17] M. Shub, *Global Stability of Dynamical Systems*, Springer-Verlag, 1987.

[18] G. Strang and G. J. Fix, *An Analysis of the Finite Element Method*, Prentice Hall Series in *Automatic Computation*, Prentice Hall, Englewood Cliffs, 1973.

Department of Mathematics and Computing Science
University of Groningen
P.O. Box 800
9700 AV Groningen
The Netherlands
E-mail: broer@math.rug.nl, osinga@cs.rug.nl, vegter@cs.rug.nl